Deep-Sea Research II 117 (2015) 23–40

Contents lists available at ScienceDirect

Deep-Sea Research II

journal homepage: www.elsevier.com/locate/dsr2

Hydrography and nutrient dynamics in the *No*rthern *So*uth *C*hina Sea *S*helf-sea (NoSoCS)

George T.F. Wong [a,b,*], Xiaoju Pan [a], Kuo-Yuan Li [a], Fuh-Kwo Shiah [a], Tung-Yuan Ho [a], Xianghui Guo [a,1]

[a] *Research Center for Environmental Changes, Academia Sinica, 128 Academia Road Section 2, Nankang, 115 Taipei, Taiwan*
[b] *Institute of Ocean and Earth Sciences, University of Malaya, Kuala Lumpur, Malaysia*

ARTICLE INFO

Available online 5 March 2015

Keywords:
South China Sea
Marginal sea
Shelf-sea
Nutrients
Internal waves

ABSTRACT

The hydrographic characteristics and the distributions of nitrate+nitrite, or (N+N), and soluble reactive phosphate, or SRP, in the *No*rthern *So*uth *C*hina Sea *S*helf-sea (NoSoCS) were determined in four transects across the shelf in the summer of 2010 and in two transects in the winter of 2011. The NoSoCS may be sub-divided into the inner shelf, the middle shelf and the outer shelf at water depths of <40 m, 40–90 m and 90–120 m, respectively. The water in the inner shelf is colder and its concentrations in the nutrients and chlorophyll-a (Chl_*a*) are higher in both seasons while the water in the outer shelf is warmer and its concentrations are lower. With depth, since the mixed layer depth in the NoSoCS in the winter ($\sim$70 m) and in the summer ($\sim$40 m) are both shallower than the shelf break depth ($\sim$120 m), the colder and relatively nutrient-rich upper thermocline-upper nutricline water in the open South China Sea (SCS) can freely extend into the NoSoCS to become its bottom water. This is a distinguishing characteristic of the NoSoCS as, unlike many of the more extensively studied temperate shelf-seas, vertical mixing within the NoSoCS, rather than shelf-edge processes such as upwelling, is the primary mechanism for bringing the nutrients from the sub-surface in the adjoining northern SCS to its mixed layer for supporting primary production. Four processes that may contribute to this vertical mixing in the NoSoCS include: shelf-wide winter surface cooling and convective mixing; the actions of internal waves which probably occur in both seasons along the entire outer shelf; wind and topographically induced coastal upwelling in the summer off Shantou at the northwestern corner of the NoSoCS; and winter formation of bottom water at the outer portion of the inner shelf and the inner portion of the middle shelf. The density of this bottom water formed in the winter of 2011 was equivalent to the density at $\sim$120 m in the open SCS so that it could cascade across the shelf and contribute to not only vertical mixing but also in cross shelf mixing and the ventilation of the upper thermocline and nutricline of the open SCS. An enrichment in (N+N) over SRP, where (N+N)/SRP exceeded the Redfield ratio of 16 and $[N+N]_{ex}>0$, was found when salinity dropped below about 33. In these fresher waters, which were found exclusively in the inner shelf during this study, SRP potentially could become the limiting nutrient.

1. Introduction

In the temperate shelf-seas, such as the more extensively studied East China Sea (Wong et al., 1991, 2004; Chen and Wang, 1999) and the South Atlantic Bight (Lee et al., 1991), the mixed layer depth in the adjoining ocean interior is often deeper than the shelf break depth. Horizontal exchange by frontal processes between the ocean interior and the shelf-sea would bring only the nutrient-poor mixed layer water from the former to the latter, and this would result in little net nutrient import into the shelf-sea. Upwelling over the shelf edge, induced by wind and/or topography, is necessary if the nutrient-laden sub-surface water below the mixed layer in the ocean interior is to be brought onto the shelf-sea to support biological activities. Since the maximum mixed layer depth in the ocean interior generally decreases with decreasing latitude (Montégut et al., 2004) while the shelf break depth, which on average is located at 130 m, is not latitude-dependent, the relationship between them and thus the availability of nutrients in the subsurface water in the ocean interior to the shelf-seas may become different in the tropical waters. Furthermore, at the lower latitudes, insolation is higher and more uniform throughout the year. The resulting water temperature in

* Corresponding author at: Research Center for Environmental Changes, Academia Sinica, 128 Academia Road Section 2, Nankang, 115 Taipei, Taiwan.
E-mail address: gtfwong@gate.sinica.edu.tw (G.T.F. Wong).
[1] *Present address*: Marine Environmental Laboratory, Xiamen University, Xiamen.

http://dx.doi.org/10.1016/j.dsr2.2015.02.023
0967-0645/

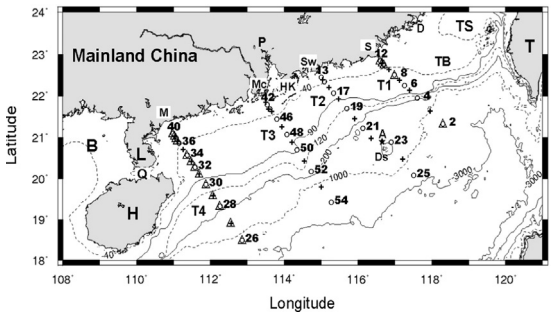

Fig. 1. The study area and the sampling locations in the Northern South China Sea Shelf-sea (NoSoCS). + – CTD stations in summer, 2010; ○ – CTD and discrete sample sampling stations in summer, 2010; Δ – CTD and discrete sample sampling stations in winter 2011. A – time series station; B – Beibu Gulf; D – Dongshan; Ds – Dongsha Atoll; H – Hainan Island; HK – Hong Kong; L – Leizhou Peninsula; M – Maoming; Mc – Macau; P – Pearl River; Q – Qiongzhou Strait; S – Shantou; Sw – Shanwei; T – Taiwan; TB – Taiwan Bank; TS – Taiwan Strait.

the mixed layer is higher and the vertical stratification is stronger; these would result in less effective winter convective overturn, which can also bring the nutrients in the sub-surface water to the mixed layer (Heinrich, 1962). Thus, the dynamics of the nutrients in the tropical and sub-tropical shelf-seas may be different from those in their better studied temperate counterpart.

The South China Sea, SCS, is the largest tropical marginal sea of the world. The *N*orthern *S*outh *C*hina Sea *S*helf-sea (NoSoCS) (Fig. 1), which forms the northwestern boundary of the SCS, is a tropical shelf-sea that extends approximately in a northeast to southwest direction from a ridge system at the southern end of the Taiwan Strait at about 23°N and 119°E to the northeastern coasts of the Leizhou Peninsula and the Hainan Island at about 20°N and 111°E with a length of about 750 km, and from the coast of southern China seaward to the shelf break at the 120-m isobath, with an average width of about 200 km. At its northeastern boundary, it is connected to the Taiwan Strait but free exchange is restricted by the ridge system that extends seaward from Dongshan to the Taiwan Bank. The maximum water depth along the ridge system does not exceed 40 m. Wind and topographically induced upwelling has been reported to occur off the coast from Shantou to Shanwei and at the shelf edge at the Taiwan Bank (Gan et al., 2009, 2010; Hong et al., 2011a). At its southwestern boundary, the NoSoCS is almost closed as it is connected to the Beibu Gulf only through the narrow Qiongzhou Strait between the Leizhou Peninsula and the Hainan Island. The Pearl River (Zhujiang) empties into the NoSoCS from the west with an average flow rate of 330 km^3/yr. The minimum flow of this river occurs during the winter and the maximum flow is reached in the summer in around July (Guo et al., 2008). Its drainage basin is highly urbanized and its water is noted for its high concentrations of organic substances and the nutrients (Chen et al., 2004; Yin et al., 2004; Yin and Harrison, 2008; Zhang, 1995). Thus, Chen (2005) and Chen and Chen (2006) suggested that the discharge of the Pearl River may play a significant role in controlling the primary production and new production in the NoSoCS. At its seaward boundary, the NoSoCS is bordered by a boundary current that flows towards the southwest in the fall through the spring and towards the northeast in the summer in response to the forcing of the monsoonal winds (Gan et al., 2006). Internal waves generated around the Luzon Strait regularly find their way to the entire outer-shelf of the NoSoCS (Guo et al., 2012). In fact, some of the largest internal waves of the world were observed around the Dongsha Atoll at the shelf edge in the northern NoSoCS (Liu et al., 2006).

Since a variety of significant oceanographic phenomena can be found in different localities within the NoSoCS, previous studies tend to focus on these sub-regions, such as the Pearl River estuary (Yin et al., 2004; Harrison et al., 2008; Yin and Harrison, 2008; Xu et al., 2009), the upwelling zones (Gan et al., 2010; Hong et al., 2011a) and the area around the Dongsha Atoll where the activities of internal waves are particularly intense (Wang et al., 2007; Pan et al., 2012). Systematic observations for a synoptic study on the NoSoCS have been rare. In order to fill this gap, we conducted two cruises to the NoSoCS in the summer of 2010 and the winter of 2011 to examine the spatial and seasonal variability in the hydrographic characteristics and in the dynamics of the nutrients in this shelf-sea. The results are reported here.

2. Experimental

2.1. Sampling

The NoSoCS was sampled in four approximately evenly spaced cross-shelf transects perpendicular to the coastal line from the coast to the open northern SCS off Shantou, Shanwei, Macau and Maoming aboard R/V Ocean Researcher I during cruise CR929 in the summer on June 2 to June 15, 2010 (Fig. 1). In the inner shelf in less than 40 m of water, stations were occupied at every 7.5 km. In the middle shelf at water depths of 40 to 90 m, the stations were 20 km apart. Further offshore, at a spacing of 30–50 km, the stations were even farther apart. At each station, the distributions of temperature and salinity, fluorescence, and, photosynthetically available radiation (PAR) were recorded with a SeaBird model SBE9/11 conductivity-temperature-depth (CTD) recorder, a Chelsea Aqua fluorometer, and, a Chelsea PAR sensor. Discrete water samples were collected at every other station with GO-FLO bottles mounted onto a Rosette sampling assembly (General Oceanic). In addition, at Station A at a location northeast of the Dongsha Atoll, the distributions of temperature, salinity, fluorescence and PAR were recorded hourly and discrete water samples were collected once every two hours over a 36 h period.

In the winter of 2011, the transect off Maoming and the inner and middle shelf in the transect off Shantou were re-occupied on board R/V Ocean Researcher I during cruise CR953 on December 29, 2010 to January 8, 2011. The distributions of temperature, salinity, fluorescence and PAR were recorded and discrete water samples were collected at all the stations.

Sub-samples were drawn from the discrete samples, quick-frozen with liquid nitrogen on board ship, and returned to a shore-based laboratory for the determination of nitrite, nitrate plus nitrite, or (N+N), and soluble reactive phosphate, SRP.

2.2. Analytical method

Nitrite and (N+N) were determined by the standard pink azo dye method which has been adapted for use with a flow injection analyzer (Strickland and Parsons, 1972; Pai et al., 1990). SRP was determined manually with the standard phosphomolybdenum blue method (Strickland and Parsons, 1972). The precisions for the determinations of nitrite, (N+N) and SRP were ± 0.03, ± 0.3 and ± 0.01 μM, respectively. The detection limits were about three times the corresponding precisions. Low level SRP in the mixed layer waters was determined by the molybdenum blue method after a pre-concentration by a co-precipitation with magnesium hydroxide (Karl and Tien, 1992; Rimmelin and Moutin, 2005). The detection limit was about 0.01 μM and the precision was about $\pm 3\%$.

2.3. Remotely sensed observations

Daily and monthly mean night time (4 μm) sea surface temperature (SST) and the concentration of chlorophyll-*a* (Chl_*a*) between July 2002 and December 2011, with a pixel size of 4×4 km^2, were derived from Level-3 products (reprocessing version R2010.0) of the MODerate Resolution Imaging

Spectroradiometer on Aqua (MODIS-Aqua) that were obtained from the NASA Ocean Color Web (http://oceancolor.gsfc.nasa.gov/). Mean images of 8-day composites of Chl_*a* were calculated arithmetically from their daily images. It is recognized that the accuracy of the remotely sensed Chl_*a* in the case 2 water in the inner shelf, as derived by using the standard ocean color algorithms (e.g. OC4 version 6), were likely to be questionable without regional tuning (International Ocean-Colour Coordinating Group (IOCCG), 2000; O'Reilly et al., 1998, 2000; Pan et al., 2008; Szeto et al., 2011). They were used here only as a qualitative indicator for pattern recognition. Weekly wind vectors, at a spatial resolution of $\sim 25 \times 25$ km^2 per pixel, were extracted from the Remote Sensing Systems (http://www.ssmi.com/windsat/) of the WindSat.

3. Results and discussion

3.1. Hydrographic characteristics of the NoSoCS and their seasonal variability

3.1.1. Summer, 2010

The wind in the NoSoCS was weak, mostly <7 m s^{-1}, and variable, ranging from the northeast to the south, in May and June and became stronger, reaching 10 m s^{-1}, and consistently from the south to southwest in July (Fig. 2a). The extensive terrestrial influence along the coast, which defines the inner shelf, was evidenced by a strip of water with abruptly higher Chl_*a* (>1 mg m^{-3}) (Fig. 2c). The outer edge of this strip appeared as a front that generally followed the 40-m isobaths and served as a demarcation of the boundary between the inner shelf and the middle shelf. The signal of the input of freshwater from the Pearl River was limited in May and June. While there was a patch of water with particularly high Chl_*a* (>5 mg m^{-3}) at the mouth of the Pearl River in May (Fig. 2c), it was generally restricted to the inner shelf, suggesting that the outflow from the Pearl River was small enough that its influence beyond the inner shelf was not clearly evident. Indeed, the discharge of the Pearl River in March to May of 2010 was 30% lower than the climatological average (Guo and Wong, 2015). In June, this patch of chlorophyll-rich water became larger but it was still confined to the inner shelf. The size of the plume reached a maximum in July when it extended northeastward into the middle shelf, suggesting that the peak discharge from the Pearl River occurred in July 2010 as in the climatological record (Guo et al., 2008). In the 8-day composites of the remotely sensed chlorophyll-*a* (data not shown here), a prominent Pearl River plume did not become evident until the first part of July. Thus, the sampling period, June 2–15, fell at the tail end of the inter-monsoonal season, before the southwest monsoon was firmly established and the arrival of the high runoff period in 2010, and, after a relatively dry Spring.

Sea surface temperature generally increased seaward (Fig. 2b) but it also increased with time between May and July 2010. In the inner shelf, the temperatures were mostly <25 °C in May, mostly >26 °C in June and mostly >28 °C in July. The distribution of temperature across the shelf did not provide particularly clear demarcation lines for distinguishing the water among the hydrographic sub-divisions in the study area as the increase in temperature across the shelf was gradual and variable. Generally colder water with elevated Chl_*a* was also found at the Taiwan Bank in the outer shelf just beyond the NoSoCS, probably as a result of the topographically induced upwelling in this area (Hong et al., 2011a).

The relationship between potential temperature, θ, and salinity, S, at each station across the transects and the surface distributions of the hydrographic properties across approximately the middle of the NoSoCS along transect T3 are shown in Figs. 3 and 4. Based on its hydrographic characteristics, the NoSoCS may be sub-divided into the inner, middle and outer shelf at water depths of <40 m, 40–90 m, and 90–120 m. The open northern SCS was found in waters with depths exceeding 120 m and its θ–S relationship followed those reported previously (Wong et al., 2007a, b). Thus, salinity increased from the surface water ($S<34.0$; $\theta>25$ °C; $\sigma_\theta<23$) to a maximum ($S\approx34.6$; $\theta\approx18$ °C; $\sigma_\theta\approx25.2$) at about 130 m at the core of the Tropical Water. It then decreased to a minimum at 400 m ($S\approx34.4$; $\theta\approx8$ °C; $\sigma_\theta\approx26.7$) in the North Pacific Intermediate Water before it increased again with depth to the deep and bottom water. As shown in the surface distributions along transect T3 (Fig. 4), the water in the inner shelf was usually

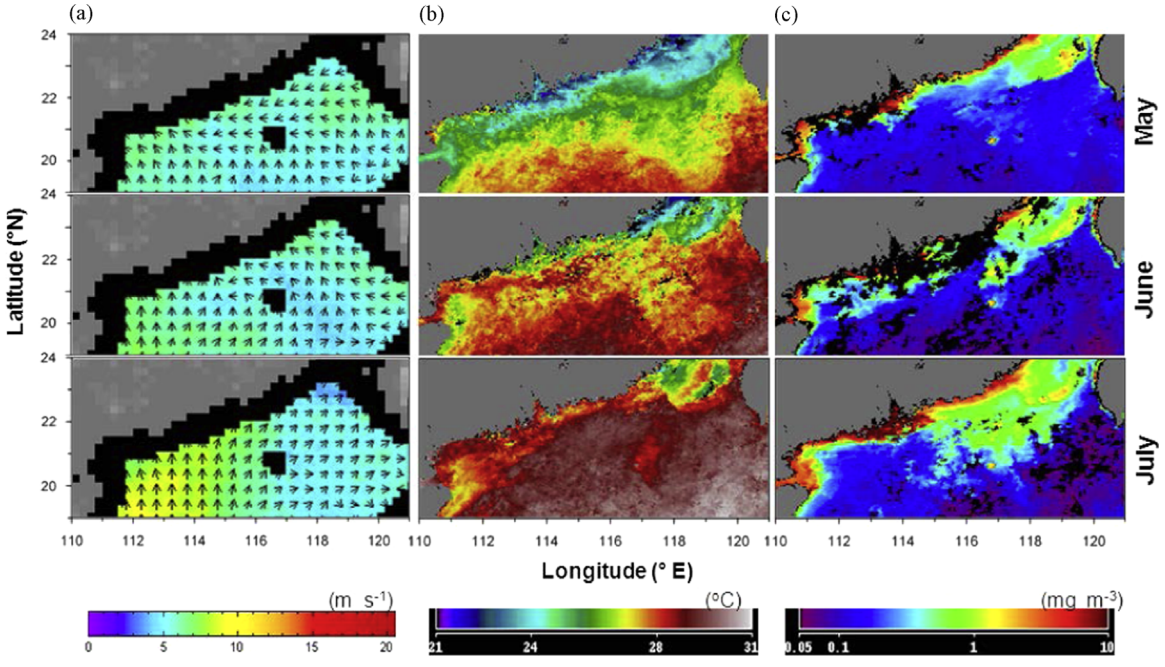

Fig. 2. The distributions of the monthly average (a) wind vector, (b) sea surface temperature (SST) and (c) surface chlorophyll-*a* concentration (Chl_*a*) in May, June and July, 2010 in the NoSoCS. Wind data from WindSat (http://www.ssmi.com/windsat/); SST and Chl_*a* data from MODIS-Aqua (http://oceancolor.gsfc.nasa.gov/).

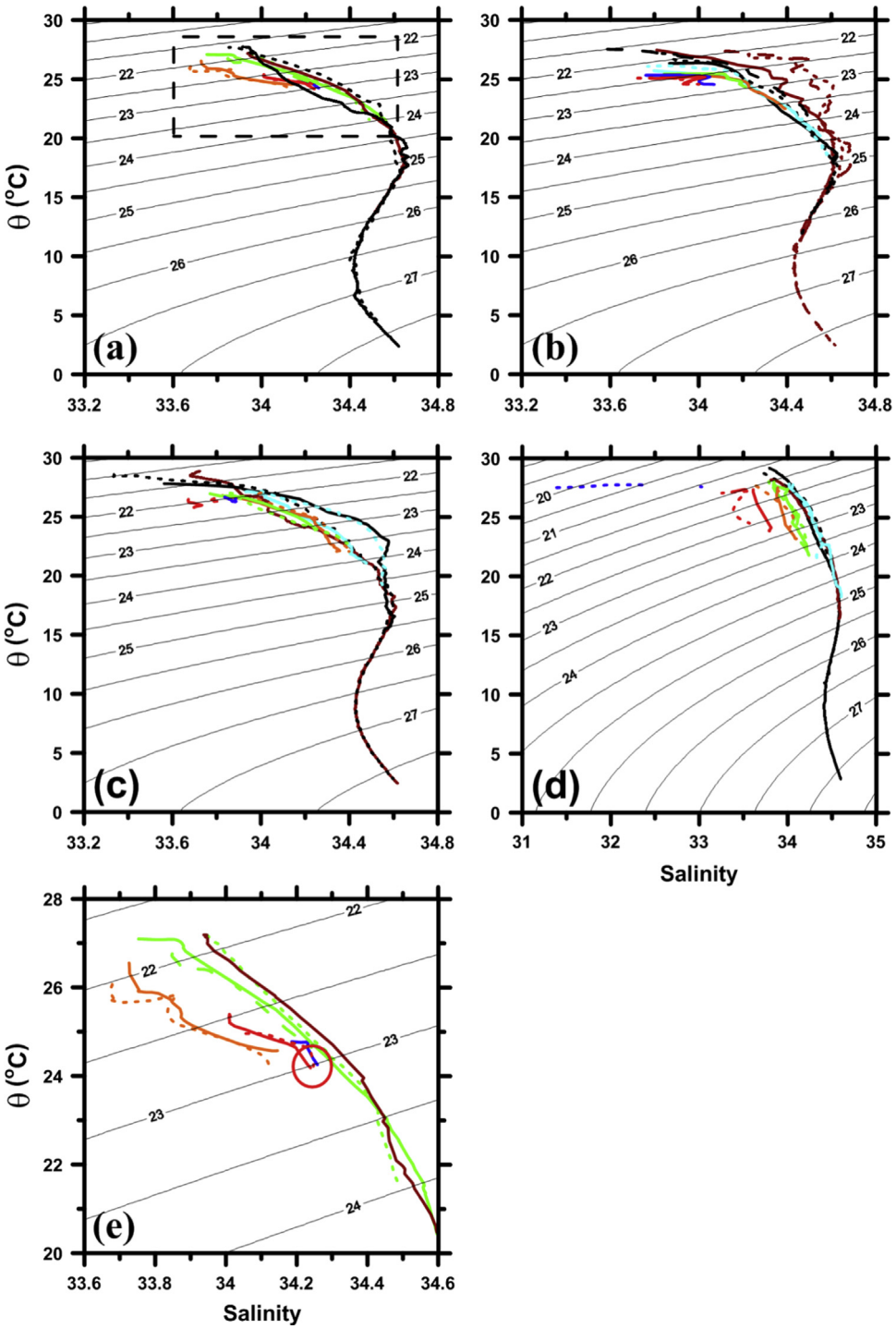

Fig. 3. The relationship between potential temperature (θ) and salinity at each station across the shelf in transect (a) T1, (b) T2, (c) T3 and (d) T4 in the summer, 2010. (e) An expanded view of the box in (a). Red and blue – inner shelf; green and orange – middle shelf; light blue – outer shelf; black and brown – open northern SCS; red circle – the point of convergence of θ–S relationships in the inner and middle shelf. (For interpretation of the references to color in this figure legend, the reader is referred to the web version of this article.)

characterized by lower temperature and salinity and higher Chl_*a*. Nevertheless, temperature and salinity rarely dropped below 25 °C and 33 (Fig. 3) and the elevations in the concentrations of the nutrients were minimal. Furthermore, the water column in the inner shelf was relatively well mixed and its θ–S relationship was frequently distinctly decoupled from those in the open northern SCS (Fig. 3). These characteristics reflect the significant terrestrial influence and the limited direct oceanic influence on the water in the inner shelf. In contrast, the water in the outer shelf was warm and saline, reaching 27 °C and 34, and its concentrations in the nutrients and chlorophyll-*a* were low. The θ–S relationship converged with that in the open northern SCS at around the core of the Tropical Water (Fig. 3), indicating that mixing with the upper water in the open northern SCS was an important determining factor of the hydrographic properties in the surface waters in this region. The middle shelf water was a mixture of the inner shelf and the outer shelf water.

The vertical distributions of potential temperature, salinity and potential density along the transects are shown in Fig. 5. The mixed layer depth, defined as the depth at which the density

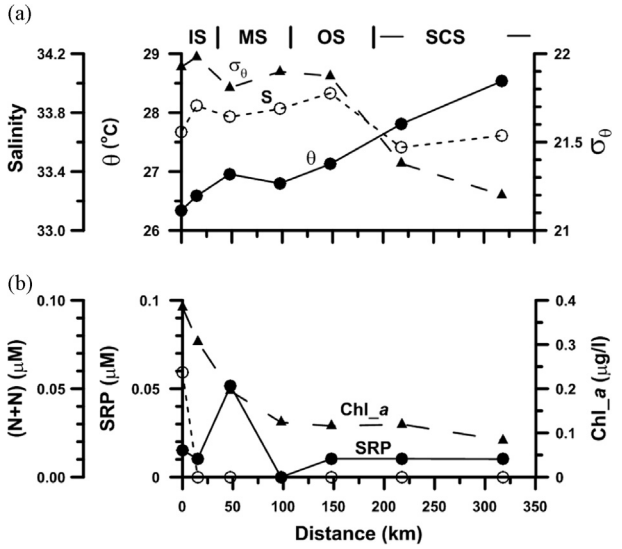

Fig. 4. The distributions of (a) potential temperature (θ, •), salinity (S, ○), potential density (σ_θ, ▲), and (b) SRP (•), (N+N) (○) and chlorophyll-*a* (Chl_*a*, ▲) in the surface water across the shelf in transect T3 off Macau in the summer, 2010. IS – inner shelf; MS – middle shelf; OS – outer shelf; SCS – open northern South China Sea.

gradient reached 0.1σ_θ unit m^{-1} (Tseng et al., 2007; Wong et al., 2007b), varied mostly between 25 and 45 m. The bottom of the mixed layer could be marked approximately by the isotherm at 25 °C, the isohaline of 34 and the isopycnal of 22 at a depth of approximately 40 m. Since the mixed layer depth was shallower than the shelf-break depth (~120 m), a layer of colder and more saline sub-surface upper thermocline water could freely extend from the open SCS into the shelf below the mixed layer and covered the bottom of the entire middle and outer shelf. Thus, with depth, as a first approximation, the NoSoCS was a two layer system: a layer of warmer (>25 °C) and fresher (<34) mixed layer water overlying a layer of colder (<25 °C) and more saline (>34) deep water.

A summary of the average hydrographic properties in these different hydrographic sub-divisions in the NoSoCS is listed in Table 1. In the mixed layer, temperature decreased systematically from 27.0 °C in the open SCS to 25.8 °C in the inner shelf. In contrast, salinity first increased from 34.0 in the open SCS to a maximum of 34.1 in the outer shelf before it decreased shoreward to 33.7 in the inner shelf. As a result, the density of the water in the NoSoCS (σ_θ=22.2) was actually higher than that in the open northern SCS (σ_θ=21.9) and the densest water was found in the outer and the middle shelf.

Superimposed on these general hydrographic characteristics were several additional sub-regional features. In the inner shelf in the northern most transect, T1, off Shantou, there was a conspicuous shoreward and upward tilting of the isotherms, isohalines and isopycnals from the middle shelf to the inner shelf (Fig. 5a). For example, the 25 °C isotherm, 34 isohaline and 22.5 isopycnal were at a depth of about 50 m off the shelf break and they reached the sea surface in the inner shelf. This is indicative of the occurrence of wind and topographically induced coastal upwelling which has been observed in this general area in the summer (Gan et al., 2009, 2010; Hong et al., 2011b) and it led to the presence of the colder (~26.7 °C) and more saline (~34) mixed layer water in the inner shelf off the coast of Shantou. In fact, along this transect T1, the salinity in the inner shelf was higher than those further offshore. The extensions of the θ–S relationships at the stations in the inner shelf converged with each other and with those further offshore in the middle shelf at about a salinity of 34.2, a temperature of 24 °C and a density of 23 (Fig. 3e). This point of convergence represented the source water of the upwelling and it could be traced to a depth of about 50 m in the middle and outer shelf. This was a relatively shallow depth, being barely below the mixed layer at the top of the thermocline.

Along the bottom of the mixed layer, an undulation of the isopleths could be detected at all four transects (Fig. 5). The undulation was gentler, with an amplitude of ~20 m, at the northern most transect T1 (Fig. 5a), and, the strongest, with an amplitude of ~50 m at transect T2 around the Dongsha Atoll (Fig. 5b). The apparent wavelengths varied between <50 and >100 km and tended to decrease landward from the open northern SCS to the middle shelf. These were of course not true wavelengths as the stations were not occupied synchronously along these transects. At the time-series Station A north of the Dongsha Atoll, the periods of these undulations were clearly shown to be about 12 h (Fig. 6). The amplitude was not constant as it varied between 30 and 50 m. The characteristics of these undulations were consistent with the effects of the activities of internal waves along the entire outer and middle shelf of the NoSoCS, with the strongest occurring in transect T2 in the vicinity of the Dongsha Atoll as reported previously (Guo et al., 2012). The undulations of the isohalines brought the saline sub-surface water to the mixed layer. This could have accounted for the slightly higher average salinity and potential density in the mixed layer in the outer and/or middle shelf in comparison to those further inshore or offshore (Table 1), and, for the higher average salinity in the mixed layer in the outer shelf in transect T2 in comparison to those in the other three transects.

In transect T4 off the coast of Maoming, the θ–S relationships in the inner, middle and outer shelf were distinctly isolated from each other (Fig. 3d). Within the inner shelf, the θ–S relationship at the most landward station was especially dissimilar from those of the other stations. The water was particularly fresh and the surface salinity dropped to as low as 28.3. All these characteristics were consistent with the influence of a local, likely terrestrial, source of fresh water.

3.1.2. *Winter, 2011 and inter-seasonal comparison*

By December 2010, the northeast monsoon had already been established firmly. Consistent and strong, mostly around 10 m s^{-1}, northeast wind covered the entire region (Fig. 7a). These wind speeds were significantly higher than those in the previous summer. Again, temperature increased while Chl_*a* decreased seaward (Fig. 7b and c). The boundary between the inner shelf and middle shelf was generally marked by the isotherm of 18 °C and the isopleth of Chl_*a* of 2 mg m^{-3}, which ran roughly along the 40-m isobath. Somewhat higher Chl_*a* were found at the mouth of the Pearl River but these elevated concentrations were confined to the inner shelf, reflecting the limited outflow from the River in the winter (Guo et al., 2008). A patch of water with lower temperatures and higher Chl_*a* was again found to associate with the Taiwan Bank. While these distributional patterns in temperature and Chl_*a* in the NoSoCS were similar to those in June 2010, their magnitudes differed. The temperatures were of course generally lower in the winter, mostly >26 °C in June and <25 °C in December/January, while the Chl_*a* were generally higher, mostly <0.5 mg m^{-3} in June and mostly >1 mg m^{-3} in December/January. A similar pattern of elevated Chl_*a* in the winter had been reported in the open northern SCS and it was attributed to the enhancement in biological productivity supported by an increase in the supply of nutrients to the surface mixed layer by the intensified vertical mixing induced by surface cooling and the action of the stronger northeast monsoon (Tseng et al., 2005). Chen and Chen (2006) found higher primary

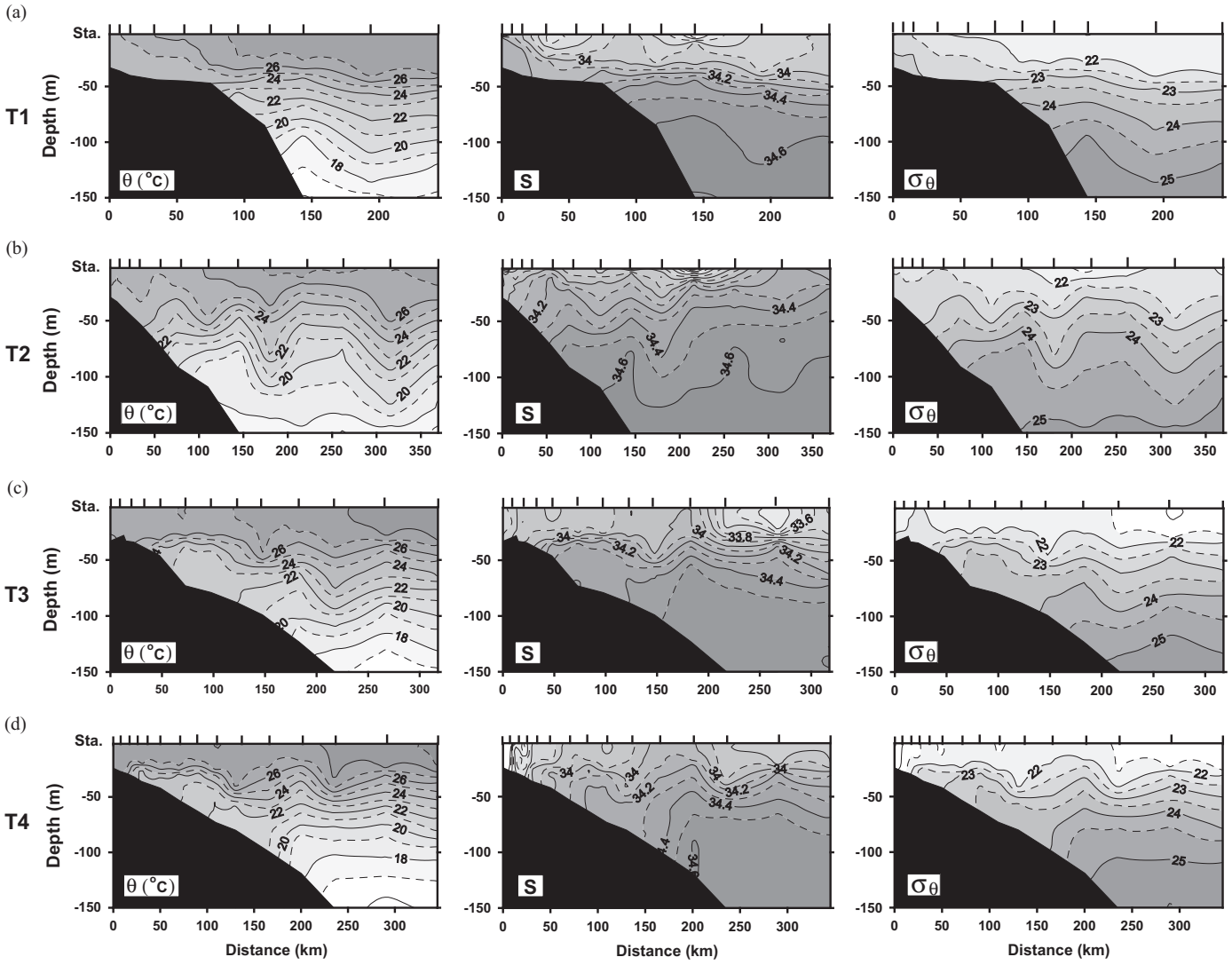

Fig. 5. The vertical sections of potential temperature (θ), salinity (S) and potential density (σ_θ) across the shelf in transects (a) T1, (b) T2, (c) T3 and (d) T4 in the summer, 2010. Locations of the stations are shown at the top of the figures as tick marks.

production and new production in the winter in the NoSoCS as well as the open northern SCS and attributed them to enhanced vertical advection in the winter.

Samples were collected only along transect T4 and in the inner shelf and part of the middle shelf along transect T1 in winter 2010 (Figs. 1 and 8). In the surface mixed layer, the average salinity in the NoSoCS was similar to that in the open northern SCS while the temperature was 2.6 °C colder and the density was 0.7σ_θ unit higher (Table 1). Within the NoSoCS, the average temperature decreased systematically shoreward from 24.7 °C in the open northern SCS to 18.3 °C in the inner shelf while salinity increased from 33.9 in the open SCS to a maximum of 34.0 in the outer shelf before it decreased to 33.1 in the inner shelf. Relative to the previous June, for the NoSoCS as a whole, the temperature in the mixed layer was lowered by 3.9 °C. The decrease was especially pronounced in the inner shelf where temperature dropped by 7.5 °C.

In the vertical section along transect T4 (Fig. 8), the bottom of the mixed layer was located at about 70 m off the shelf and it could be marked generally by the 24 °C isotherm, 34 isohaline and 23 isopycnal. The entire water column in the inner shelf and in most of the middle shelf was well mixed. In comparison to the summer, the mixed layer depth had deepened by about 30 m. However, since the mixed layer depth was still shallower than the shelf-break depth, the colder and more saline upper thermocline water could still extend freely into the outer and part of the middle shelf and underlie the mixed layer as in the summer. Also as found in the summer, the θ–S relationships (Fig. 9) at the stations in the outer shelf fell on the same trend as those in the open northern SCS. However, in the inner shelf, the relationships were decoupled from those further offshore. In the middle shelf, the θ–S relationships indicated mixing between the warm and saline surface water in the outer shelf with a mass of fresher ($S = \sim 33.7$), colder ($= \sim 21$ °C) and denser ($\sigma_\theta = \sim 23.4$) water which occupied the entire water column of the inner portion of the middle shelf (Fig. 8). This water was the densest water along the entire transect. Further offshore, it continued as a tongue of dense, cold and fresh bottom water that extended seaward across the NoSoCS towards the open northern SCS. The isopycnal at 23.4 could be tracked to about 80 m in the upper thermocline offshore. Along transect T1, the maximum density was found in the inner shelf and it reached a value of 24.6, which was equivalent to that at about 120 m in the open northern SCS. The corresponding temperature and salinity of this water was 18.5 °C and 34.3. This salinity was unusually high among the surface waters and could only originate from the saline subsurface Tropical Water off the shelf. These suggest that the

Table 1
Average hydrographic properties and concentrations of nutrients and chlorophyll-*a* in the hydrographic sub-divisions in the Northern South China Sea Shelf-sea.

	Northern South China Sea Shelf-sea[a]							Open SCS[a]	
	Inner Shelf	Middle Shelf		Outer Shelf		Whole Shelf-sea			
June 2010 (Summer)									
Depth range (m)		< 40	> 40	< 40	> 40	< 40	> 40	< 40	40–120
Area (10^4 km^2)	6.50	6.78	6.78	2.83	2.83	16.11	9.61	–	–
Volume (10^3 km^3)	1.12	2.71	1.51	1.13	1.60	4.97	3.11	–	–
S	33.7 ± 0.7 (428)	34.0 ± 0.2 (603)	34.3 ± 0.1 (300)	34.1 ± 0.1 (189)	34.4 ± 0.1 (297)	33.9 ± 0.3 (1220)	34.4 ± 0.1 (597)	34.0 ± 0.3 (594)	34.5 ± 0.1 (1276)
T (°C)	25.8 ± 1.1 (428)	26.0 ± 1.3 (603)	22.8 ± 1.1 (300)	26.1 ± 1.2 (189)	21.6 ± 2.1 (297)	26.0 ± 1.3 (1220)	22.2 ± 1.6 (597)	27.0 ± 1.2 (594)	21.2 ± 2.4 (1276)
σ_θ	22.1 ± 0.8 (428)	22.3 ± 0.5 (603)	23.5 ± 0.4 (300)	22.3 ± 0.5 (189)	23.9 ± 0.7 (297)	22.2 ± 0.6 (1220)	23.7 ± 0.5 (597)	21.9 ± 0.6 (594)	24.0 ± 0.7 (1276)
SRP (μM)	0.06 ± 0.06 (33)	0.04 ± 0.04 (34)	0.21 ± 0.07 (10)	0.01 ± 0.01 (13)	0.27 ± 0.24 (9)	0.04 ± 0.04 (80)	0.24 ± 0.16 (19)	0.02 ± 0.03 (28)	0.40 ± 0.23 (27)
N+N (μM)	1.0 ± 3.1 (33)	0.05 ± 0.12 (34)	1.7 ± 1.4 (10)	0.00 ± 0.01 (13)	3.0 ± 3.3 (9)	0.3 ± 0.8 (80)	2.3 ± 2.4 (19)	0.05 ± 0.14 (28)	5.3 ± 3.6 (27)
Nitrite (μM)	0.2 ± 0.7 (33)	0.01 ± 0.03 (34)	0.4 ± 0.4 (10)	0.00 ± 0.00 (13)	0.10 ± 0.08 (9)	0.05 ± 0.18 (80)	0.24 ± 0.27 (19)	0.01 ± 0.03 (28)	0.10 ± 0.11 (27)
Chl (μg l^{-1})	0.68 ± 0.56 (33)	0.50 ± 0.49 (31)	0.56 ± 0.23 (9)	0.21 ± 0.12 (9)	0.32 ± 0.19 (9)	0.47 ± 0.42 (73)	0.44 ± 0.21 (18)	0.23 ± 0.18 (26)	0.23 ± 0.16 (27)
Fl	0.35 ± 0.27 (428)	0.16 ± 0.16 (603)	0.33 ± 0.12 (300)	0.13 ± 0.10 (189)	0.21 ± 0.11 (297)	0.20 ± 0.17 (1220)	0.27 ± 0.11 (597)	0.10 ± 0.08 (594)	0.15 ± 0.10 (1276)
December 2010/January 2011 (Winter)									
Depth range (m)		< 70	> 70	< 70	> 70	< 70	> 70 m	< 70	70–120 m
Area (10^4 km^2)	6.50	6.78	2.92	2.83	2.83	16.11	5.75	–	–
Volume (10^3 km^3)	1.12	4.02	0.20	1.98	0.75	7.13	0.95	–	–
S	33.1 ± 0.9 (144)	33.9 ± 0.2 (322)	33.63 ± 0.03 (7)	33.97 ± 0.08 (133)	34.2 ± 0.2 (45)	33.8 ± 0.3 (599)	34.1 ± 0.2 (52)	33.9 ± 0.3 (269)	34.4 ± 0.2 (200)
T (°C)	18.3 ± 0.5 (144)	22.0 ± 1.7 (322)	22.0 ± 0.2 (7)	24.3 ± 0.2 (133)	23.2 ± 0.7 (45)	22.1 ± 1.1 (599)	22.9 ± 0.6 (52)	24.7 ± 0.7 (269)	21.4 ± 2.1 (200)
σ_θ	23.7 ± 0.8 (144)	23.4 ± 0.6 (322)	23.17 ± 0.08 (7)	22.8 ± 0.1 (133)	23.3 ± 0.3 (45)	23.3 ± 0.5 (599)	23.3 ± 0.3 (52)	22.6 ± 0.3 (269)	23.9 ± 0.7 (200)
SRP (μM)	0.29 ± 0.14 (10)	0.09 ± 0.05 (20)	ND	0.05 ± 0.01 (10)	0.30 ± 0.21 (3)	0.11 ± 0.05 (40)	0.30 ± 0.21 (3)	0.04 ± 0.03 (21)	0.44 ± 0.25 (8)
N+N (μM)	7.2 ± 4.9 (10)	0.7 ± 0.5 (19)	ND	0.4 ± 0.1 (10)	3.8 ± 2.8 (3)	1.7 ± 1.1 (39)	3.8 ± 2.8 (3)	0.36 ± 0.24 (21)	6.3 ± 3.8 (8)
Nitrite (μM)	2.9 ± 1.9 (10)	0.48 ± 0.56 (20)	ND	0.06 ± 0.04 (10)	0.06 ± 0.02 (3)	0.7 ± 0.6 (40)	0.06 ± 0.02 (3)	0.03 ± 0.05 (21)	0.10 ± 0.05 (8)
Chl (μg l^{-1})	0.65 ± 0.41 (10)	0.50 ± 0.16 (20)	ND	0.45 ± 0.09 (10)	0.09 ± 0.01 (3)	0.51 ± 0.18 (40)	0.09 ± 0.01 (3)	0.32 ± 0.10 (21)	0.14 ± 0.09 (8)
Fl (RFU)	0.18 ± 0.06 (144)	0.18 ± 0.05 (322)	0.08 ± 0.01 (7)	0.17 ± 0.03 (133)	0.08 ± 0.06 (45)	0.18 ± 0.05 (599)	0.08 ± ± 0.05 (52)	0.14 ± 0.06 (269)	0.06 ± 0.08 (200)

Numbers in brackets – number of data points available for calculating the standard deviations. SRP – soluble reactive phosphate; (N+N) – (nitrate+nitrite); Chl – chlorophyll-*a*; Fl – fluorescence; RFU – relative fluorescence unit; ND – no data.

[a] Uncertainties represent 1 standard deviation from the mean.

density of the bottom water formed in the NoSoCS in the winter could be dense enough that it was able to cascade across the bottom of the NoSoCS and spread into the upper thermocline in the open northern SCS. While the data were still limited, the presence of this dense water in the inner or middle shelf at both the northeastern-most and the southwestern-most transects across the NoSoCS suggests that this phenomenon of bottom water formation and intrusion into the open northern SCS might occur along the entire shelf. Tsunogai et al. (1999) hypothesized the occurrence of a similar process in the temperate East China Sea Shelf-sea for the removal of atmospheric carbon dioxide to the oceans and named it the continental shelf pump. However, this hypothesis has yet to be corroborated adequately with direct observations. Our observations provide likely one of the first evidence for its occurrence in a tropical shelf-sea. This process can enhance vertical mixing and cross shelf mixing in the shelf. Thus, it could have facilitated material exchange between the NoSoCS and the open northern SCS and the ventilation of the upper thermocline water of the adjoining northern SCS. Undulations in the isotherms, isohalines and isopycnals, which were indicative of the activities of internal waves, while less conspicuous in the winter, were still evident in the outer shelf along transect T4. Thus, the activities of the internal waves along the outer shelf might occur year round although the stronger waves were likely found in the summer as noted previously (Zheng et al., 2007). On the other hand, while the water at the coast of Maoming in transect T4, with a salinity of 31.8, was still relatively fresh, it was not nearly as fresh as that (S=28.3) found in June. This was consistent with the drier condition and the reduced terrestrial freshwater outflow to the NoSoCS in the winter.

3.2. Distributions of dissolved (N+N), SRP and nitrite – seasonal characteristics and variability

3.2.1. Summer 2010

The top of the nutricline depth (~40 m) in summer 2010 was located at about the same depth as the bottom of the mixed layer (Fig. 10). (The top of the nutricline depth is defined as the depth corresponding to the temperature at which the concentrations of the nutrients reached zero in the linear regression relationship between the nutrient concentrations and potential temperature.) Thus, the mixed layer of the NoSoCS was almost devoid of nutrients and nutrient availability could have been a major control on primary production in the mixed layer. On the other hand, the euphotic zone depth was at 60–80 m seaward of the middle shelf but it dropped to 25–50 m in the inner shelf. (The euphotic zone

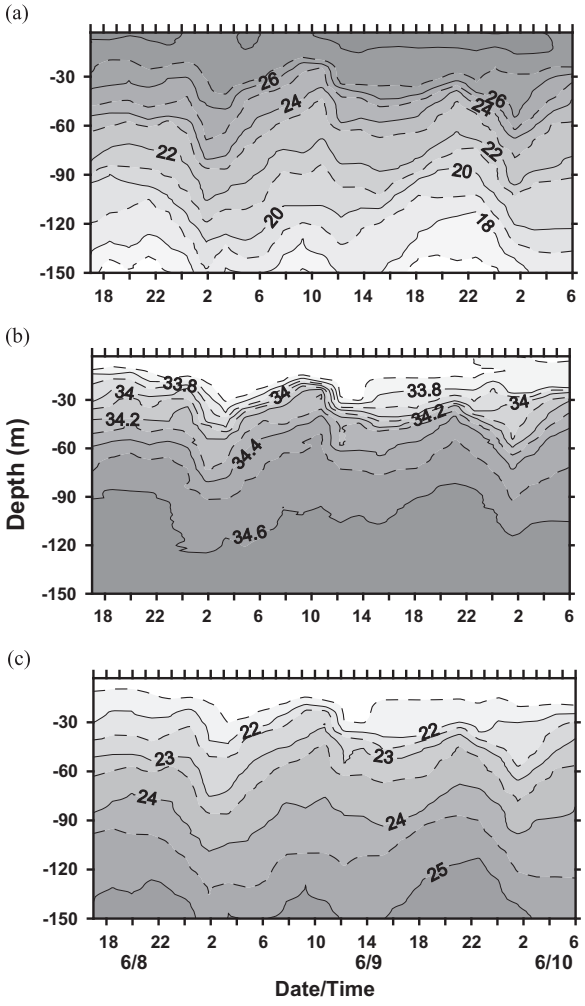

Fig. 6. Temporal variations in the distributions of (a) potential temperature (θ), (b) salinity (S) and (c) potential density (σ_θ) at Station A over 36 h. The times at which the station was sampled are shown at the top of the figures as tick marks.

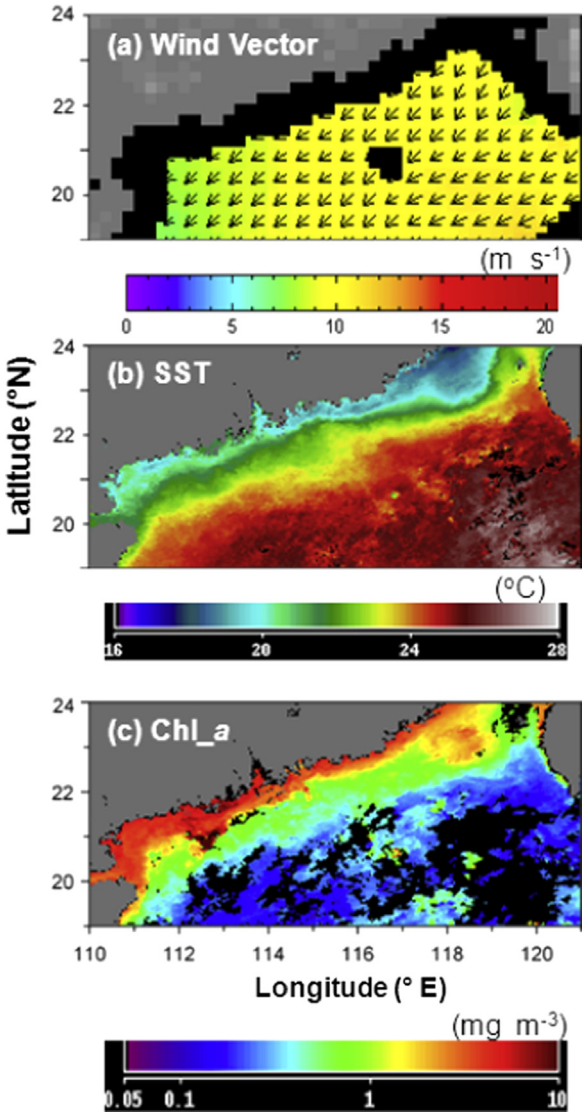

Fig. 7. The distributions of monthly average (a) wind vector, (b) sea surface temperature (SST) and (c) surface chlorophyll-*a* concentration (Chl_*a*) in December 2010 in the NoSoCS.

depth is the depth at which the light intensity dropped to 1% of the intensity of the incident light at the sea surface as projected from the relationship between photosynthetically active radiation and depth.) Thus, except at a few specific locations in the inner shelf, since the euphotic zone depth was generally deeper than the mixed layer depth, light was readily available and was not a limiting factor of primary production in the mixed layer of the NoSoCS as reported by Chen (2005) and Chen and Chen (2006).

In the mixed layer, the concentrations of SRP, (N+N) and nitrite were higher, at 0.04 μM, 0.3 and 0.05 μM, in the NoSoCS as a whole than those, at 0.02 μM, 0.05 and 0.01 μM respectively, in the open northern SCS (Table 1). Within the NoSoCS, their concentrations increased towards the coast, reaching 0.06, 1 and 0.2 μM in the inner shelf. Below the mixed layer, the upper nutricline water from the open SCS extended freely into the shelf to become a layer of moderately nutrient-rich bottom water, with average concentrations of SRP and (N+N) of 0.2 and 2 μM (Table 1), lining the entire NoSoCS (Fig. 10). Horizontal mixing along isopycnals in this layer of water will bring nutrients in the upper nutricline of the adjoining open SCS to the NoSoCS. Vertical mixing within the NoSoCS may then bring the nutrients to the mixed layer to support primary production in the NoSoCS. Thus, shelf-edge upwelling over the shelf break may not be required for providing nutrients to the NoSoCS, as is reported in many of the more extensively studied temperate shelf-seas where the mixed layer depth off the shelf is similar to or even deeper than the shelf break depth, (Lee et al., 1991; Wong et al., 1991, 2004; Chen and Wang, 1999). This is a distinguishing characteristic of the nutrient dynamics in the NoSoCS that differentiates it from many of the shelf-seas that have been studied to date.

The highest concentrations of (N+N), 16.2 μM, and nitrite, 1.3 μM, in the mixed layer were associated with the fresher water in the inner shelf off the coast of Maoming in transect T4. These concentrations were 16 and 6 times the average concentrations in the inner shelf (Table 1). On the other hand, the corresponding concentration of SRP, 0.08 μM, was only slightly higher than the average concentration, 0.06 μM, in the inner shelf. The resulting molar ratio of (N+N) to P in these waters, ~200, was much higher than that of 15 in average seawater. Such enrichments in nitrite and in (N+N) over SRP were not uncommon among the waters in the major Chinese rivers, including the Pearl River (Zhang, 1996; Dai et al., 2008). Liu et al. (2012) reported that the submarine ground water discharge to the NoSoCS is also enriched in (N+N) relative to SRP. The relative concentrations of the nutrients in these waters were consistent with the influence of these terrestrial sources. Nevertheless, in addition to direct input, the elevated concentrations of nitrite in the inner shelf water could also have

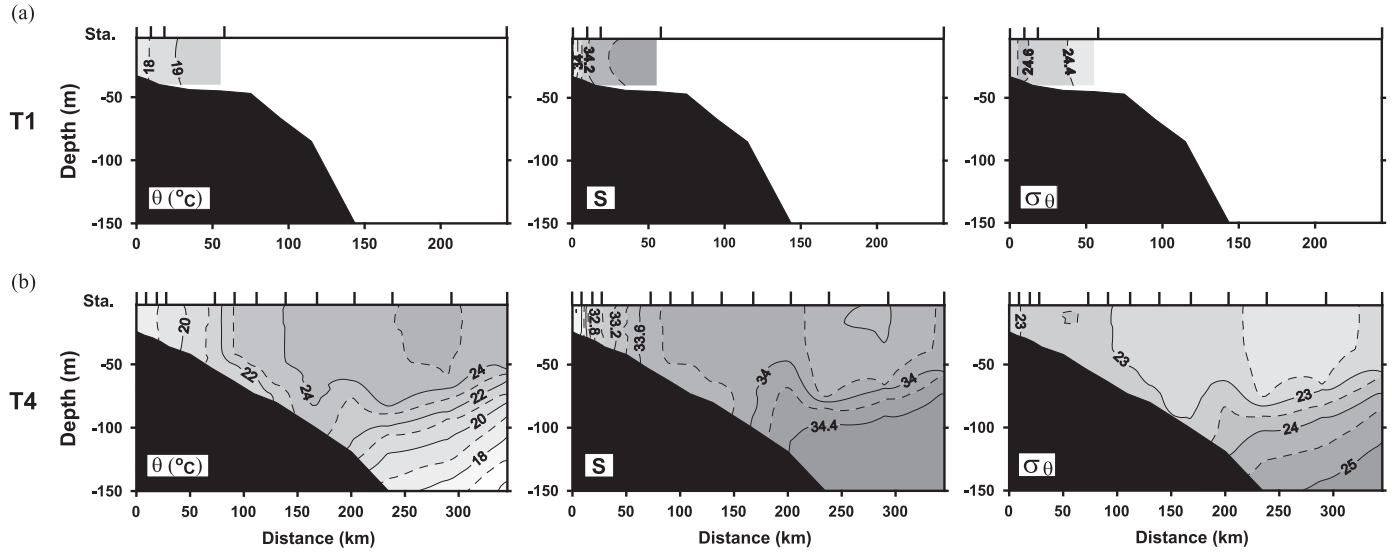

Fig. 8. The vertical sections of potential temperature (θ), salinity (S) and potential density (σ_θ) across the shelf in transect (a) T1, and (b) T4 in the winter, 2011. Locations of the stations are shown at the top of the figures.

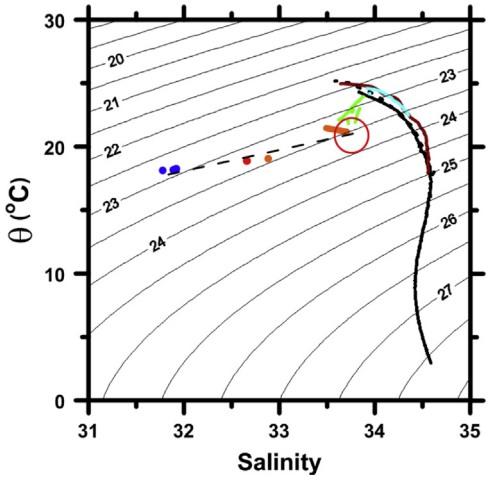

Fig. 9. The relationship between potential temperature (θ) and salinity at each station across the shelf in transect T4 in winter 2011. Red and blue – inner shelf; green and orange – middle shelf; light blue – outer shelf; black and brown – open northern SCS; red circle – point of convergence of θ–S relationships in the inner and middle shelf; long dashed line – trend of inner shelf waters. (For interpretation of the references to color in this figure legend, the reader is referred to the web version of this article.)

resulted from nitrification and/or nitrate reduction within the inner shelf and these possibilities cannot yet be ruled out.

In the sub-surface away from the inner shelf and the dominance of the influence of the terrestrial inputs, the primary nitrite maximum, which was indicative of the effect of the nitrification of organic matter, was well represented as a layer of water with concentrations of nitrite exceeding 0.05 μM that stretched across almost the entire transect just below the mixed layer between 50 and 100 m in the upper nutricline in all four transects (Fig. 10). The higher concentrations, reaching 1.1 μM, were found at the bottom of the shelf. Off the shelf, the highest concentration found was 0.5 μM. The higher concentrations on the shelf were consistent with the higher productivity in the shelf-seas which might provide a greater supply of organic matter for supporting nitrification, or, a sedimentary source.

The effect of the activities of the internal waves on the distributions of the nutrients (Fig. 10) followed those on the distributions of temperature, salinity and density (Fig. 5) closely. Thus, the isopleths of the nutrients undulated along the transects from the open northern SCS to the middle shelf. The amplitude of the undulations increased while the spacing decreased shoreward. The largest amplitude was again found along transect T2 (Fig. 10). At the time-series Station A, the isopleths of SRP and (N+N), and the location of the primary nitrite maximum undulated with a period of about 12 h and an amplitude of 30–50 m (Fig. 11). These undulations of the isopleths may facilitate the transfer of the nutrients in the sub-surface waters to the surface mixed layer and elevate primary production. Indeed, the average concentration of SRP, 0.03 μM, was higher in the mixed layer in the outer shelf in transect T2 around the Dongsha Atoll, where the activities of the internal waves were the strongest, than those in the outer shelf of the other three transects where the concentrations of SRP were only 0.01–0.02 μM. Pan et al. (2012) also reported an enhancement in the biological productivity north of the Dongsha Atoll where internal waves undergo transformation and even dissipation.

The influence of upwelling off Shantou in transect T1 on the distribution of (N+N) was not particularly conspicuous as the θ–S relationships indicated that its source water was from a rather shallow depth of about 50 m (Fig. 3e) where the concentrations of (N+N) were not expected to be highly elevated. However, by using a more sensitive method with a lower detection limit, upwelling could still be inferred from the distribution of SRP by the upward and shoreward tilting 0.05 μM isopleth which reached the sea surface in the inner shelf (Fig. 10).

3.2.2. *Winter 2011 and inter-seasonal comparison*

The top of the nutricline depth in winter 2011 was located at about 50 m (Fig. 12). With a shelf break depth of 120 m, the relatively nutrient-replete upper nutricline water in the open SCS could again extend freely into and cover part of the bottom of the NoSoCS. The bottom of the mixed layer was marked by the isopleths of (N+N) and SRP of 3 and 0.2 μM. The euphotic zone depth was at about 60–80 m deep in the outer shelf as in the summer but it dropped to 5–20 m in the inner shelf. Thus, light could be limiting primary production in some parts of the inner shelf. The euphotic zone depths in the inner shelf in the winter were shallower than those in the summer. The stronger wind in the winter might have led to more extensive re-suspension of particles and a thinner euphotic zone in these shallow waters.

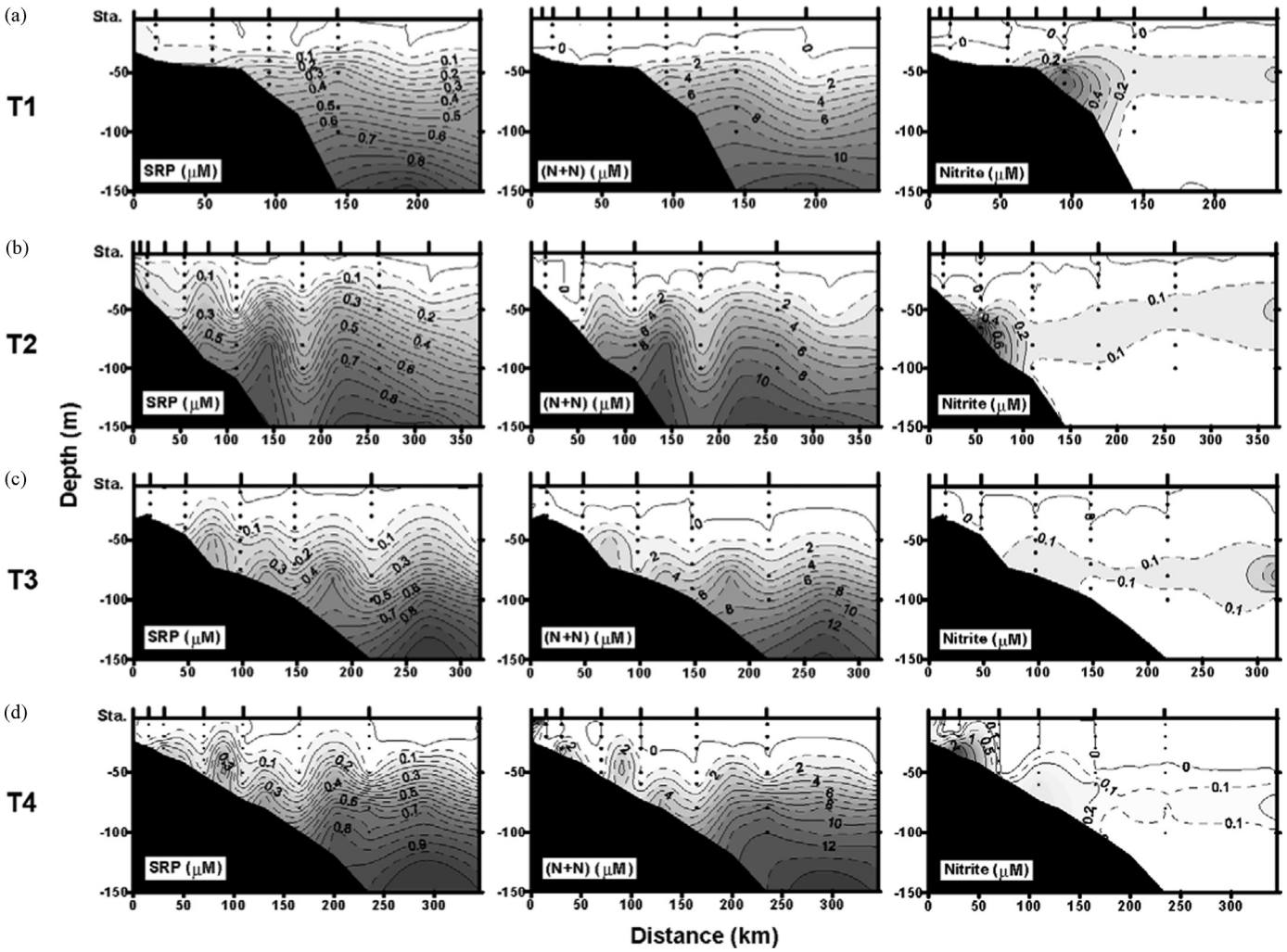

Fig. 10. The vertical sections of SRP, (N+N) (contouring augmented by concentrations from nutrient–θ relationships) and nitrite across the shelf in transects (a) T1, (b) T2, (c) T3 and (d) T4 in the summer 2010. Locations of the stations are shown at the top of the figures as tick marks.

As observed in the summer, in the mixed layer, the concentrations of SRP, (N+N) and nitrite in the NoSoCS, at 0.11, 1.7 and 0.7 μM, were higher than those, at 0.04, 0.36 and 0.03 μM, in the open northern SCS (Table 1). Within the NoSoCS, the concentrations increased towards the coast. The increases were especially noticeable between the middle shelf and the inner shelf as the average concentrations of SRP, (N+N) and nitrite increased by 3–10 times from 0.09, 0.7 and 0.48 μM to 0.29, 7.2 and 2.9 μM (Table 1). The highest concentrations, 0.49, 12.5 and 5 μM respectively, were found in the inner shelf in transect T4. In comparison to the previous summer, the average concentrations in the NoSoCS as a whole and in the open SCS were higher in the winter by a factor of 2–10. The increases in the concentrations of (N+N) and nitrite in the NoSoCS were especially conspicuous. An obvious mechanism that could have led to the elevated concentrations in the winter was convective mixing due to surface cooling as it would deepen the mixed layer and bring the nutrients in the subsurface water in the summer into the surface mixed layer. Indeed, Chen and Chen (2006) reported similar trends in the seasonal variations in the concentrations of SRP and (N+N) and suggested this winter convective mixing as the primary control on the associated seasonal variations in the primary and new production in both the NoSoCS and the open northern SCS. In this study, in the open northern SCS, between the summer and the winter, the concentrations of SRP and (N+N) in the surface mixed layer were elevated from 0.02 to 0.04 and from 0.05 to 0.36 μM respectively. Assuming a conservative behavior, the SRP and the (N+N) in the top 70 m, the thickness of the mixed layer in the winter, in the summer could yield average concentrations of 0.06 and 0.4 μM. These concentrations were similar to the observed concentrations in the mixed layer in the winter, suggesting that convective mixing could at least be a significant contributing explanation for the elevated concentrations of nutrients in the mixed layer in the open northern SCS in the winter. Indeed, Tseng et al. (2005) reported that surface cooling could account for about half of the deepening of the nutricline in the winter in the open northern SCS. The other half was attributed to the stronger winter monsoonal wind. On the other hand, in the NoSoCS, between the summer and the winter, the concentrations of SRP and (N+N) were elevated from 0.04 to 0.11 and 0.3 to 1.7 μM while convective mixing to 70 m could increase the concentrations of SRP and (N+N) only at most to 0.06 and 0.4 μM. Thus, winter convective mixing was grossly inadequate for accounting for the additional nutrients in the winter and other sources had to be in play. These sources may include increased input from the subsurface water, riverine input (Dai et al., 2008), submarine groundwater discharge (Liu et al., 2012) and sedimentary input. As reported by Tseng et al. (2005), the stronger wind in the winter could have led to a more extensive vertical mixing and an increased input of nutrients from the subsurface water. The formation of the dense deep water in the winter in the middle and/or inner shelf could also enhance material exchange between the mixed layer and the upper thermocline/nutricline

water and result in an increase in the input of nutrients to the mixed layer. The seasonal variations in the remaining three possible sources of nutrients to the mixed layer of the NoSoCS are still poorly known. It would be difficult to assess their contributions to the seasonal variations with much certainty.

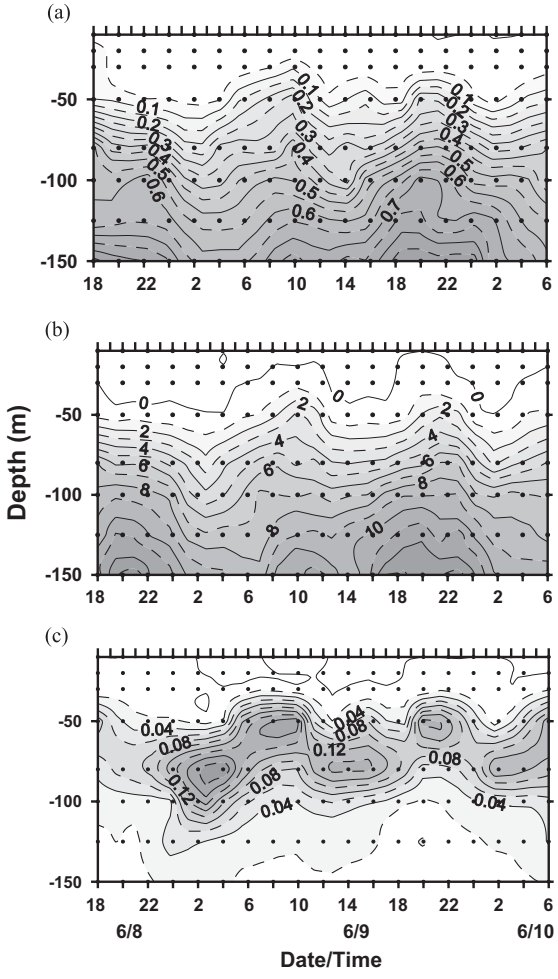

Fig. 11. Temporal variations in the distributions of (a) SRP, (b) (N+N) and (c) nitrite at Station A over 36 h. The times at which the station was sampled are shown at the top of the figures as tick marks.

3.3. Relationships among the nutrients and the physical hydrographic characteristics

The concentrations of both SRP (Figs. 13a and b) and (N+N) (relationships not shown) were both linearly related to potential temperature below about 23 °C when the data points from the inner shelf were excluded from the analyses such that:

$$\text{Summer}: \quad (\text{N+N})\ (\mu\text{M}) = -1.86(\pm 0.02)\theta + 43.5(\pm 0.3)$$
$$N = 83;\ r^2 = 0.988$$
$$\text{SRP}\ (\mu M) = -0.133(\pm 0.002)\theta + 3.15(\pm 0.02)$$
$$N = 83;\ r^2 = 0.988$$

$$\text{Winter}: \quad (\text{N+N})\ (\mu\text{M}) = -2.02(\pm 0.06)\theta + 46.7(\pm 1.0)$$
$$N = 43; \quad r^2 = 0.962$$
$$\text{SRP}\ (\mu M) = -0.140(\pm 0.004)\theta + 3.23(\pm 0.07)$$
$$N = 43; \quad r^2 = 0.965$$

These linear relationships suggest that mixing between the mixed layer water and the deep water was the primary control of the concentrations of the nutrients. Furthermore, seasonal variations in these relationships were small. They were also similar to the average relationships reported previously at the SouthEast Asian Time-series Study (SEATS) station in the northern SCS in 1999–2003 (Wong et al., 2007b). Differences in the coefficients could be attributed almost entirely to the statistical uncertainties. The agreement indicates the reliability in the quality of the data and the robustness of these relationships. (In this study, these relationships were also used for estimating the concentrations of SRP and (N+N) at stations where only CTD data were available and these estimated concentrations of the nutrients were used as supplementary guides in the construction of the vertical sections of their distributions along the transects in Fig. 10.) According to these relationships, the concentrations of (N+N) and SRP dropped to zero at around 23–24 °C, which was approximately the temperature at the bottom of the mixed layer. Superimposed on these generally linear relationships were minor inflexion points at 7 °C and 13 °C, representing the influence of the Intermediate Water

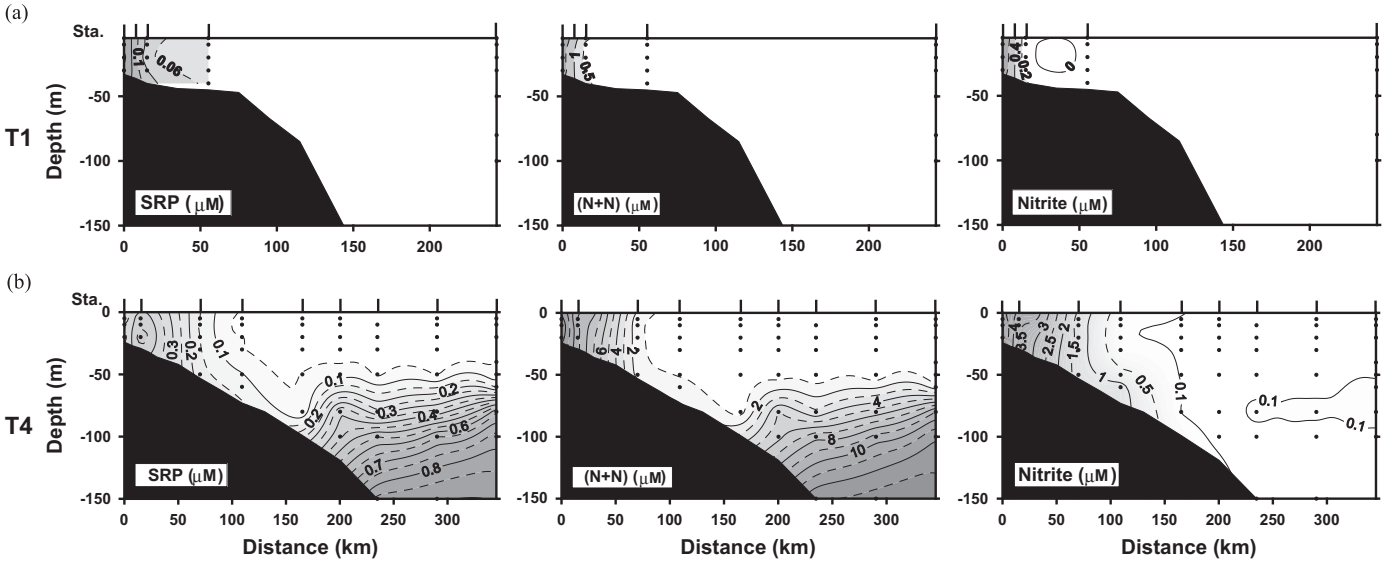

Fig. 12. The vertical sections of SRP, (N+N) and nitrite across the shelf in transect (a) T1, and (b) T4 in winter 2011. Locations of the stations are shown at the top of the figures as tick marks.

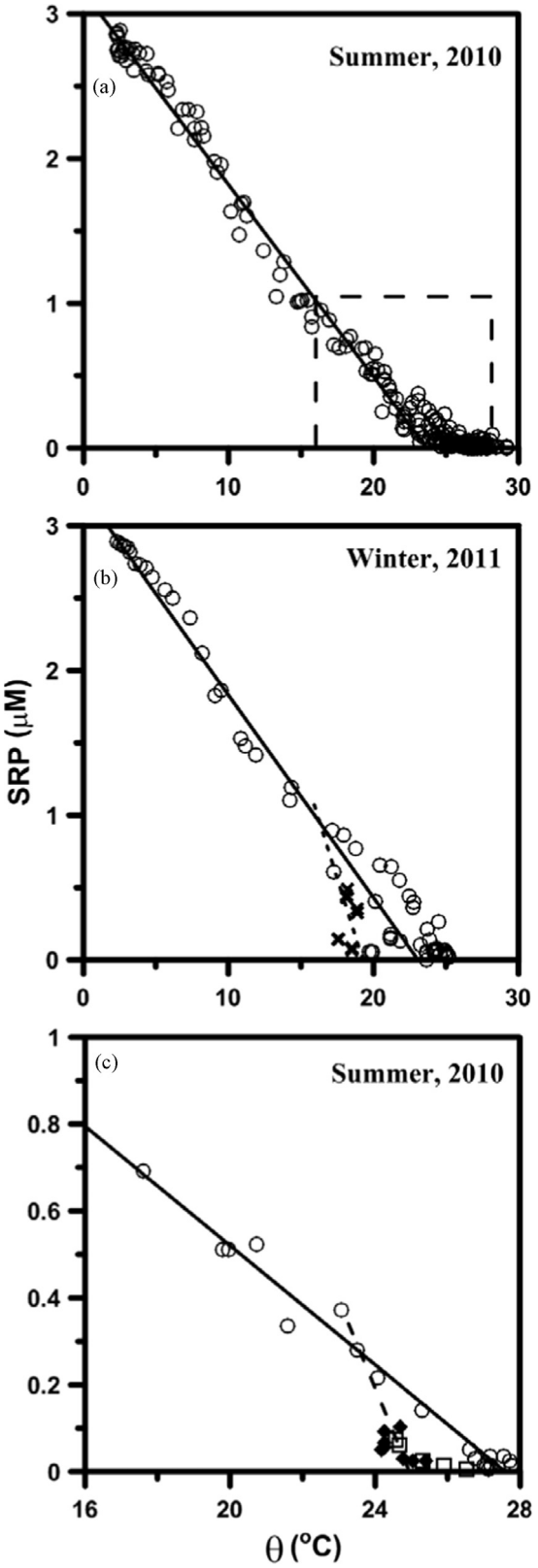

Fig. 13. The relationships between SRP and potential temperature (θ) in (a) the summer 2010; and (b) the winter 2011, x – inner shelf. (c) An expanded view of the box in (a) in transect T1, ◆ – inner shelf; □ – middle shelf; ○ – all other data points; solid line – best fit line at temperatures below 23 °C when data points from the inner shelf were excluded.

and the Tropical Water, as reported previously (Gong et al., 1992; Chao et al., 1996; Chen et al., 2001; Wong et al., 2007b).

A more detailed examination of the data points in the upper water in transect T1 in the summer indicates that the relationship between the concentration of SRP and potential temperature in the inner and middle shelf, where upwelling occurred, and in the rest of the NoSoCS followed two different but approximately linear trends (Fig. 13c). The two relationships intersected each other at about 23.5 °C, the temperature at which the θ–S relationships at the stations in the inner and middle shelf converged (Fig. 3). This point of intersection was suggestive of the source water of the upwelling and its corresponding concentrations of SRP and (N+N) were about 0.3 and 3 μM respectively. The intensity of this summer upwelling off Shantou can be irregular and ephemeral depending on the duration, direction and speed of the wind (Shang et al., 2004; Gan et al., 2009, 2010; Hong et al., 2011a). In this instance, the source water was relatively shallow and its nutrient concentrations were relatively low. As a result, the average concentration of SRP in the mixed layer in the upwelling zone in the inner shelf off Shantou, 0.06 μM, while higher than those in the middle and outer shelf, was still low and was not that dissimilar from those found in the inner shelf in the other transects. Thus, upwelling might not have been a very dominant source of nutrients to the mixed layer. In the winter, the data points from the inner and part of the middle shelf also followed a different linear trend that intersected the general trend further offshore at a temperature of about 18 °C (Fig. 13b) where the concentrations of SRP and (N+N) were about 1 and 12 μM. This relationship might have represented the mixing of the dense and homogeneous column of water in the inner and middle shelf with the upper nutricline water offshore.

The relationships between nitrite and potential density in the two seasons are shown in Fig. 14. They indicate two distinctly separated clusters of data points with higher concentrations of nitrite in each season, suggesting two different sources of nitrite associated with two different water masses. One cluster was found at around σ_θ 23 to 24 in the summer and 24.5 in the winter. It was associated with the primary nitrite maximum at 50–100 m in the outer shelf and beyond. Another cluster was found at shallower depths in the middle and inner shelf at σ_θ below 21 in the summer and below 23.5 in the winter. The highest concentrations in these clusters were frequently found in the bottom water. The nitrite in these shallower and lighter coastal waters were not related to the primary nitrite maximum and could have originated from terrestrial input or the nitrification of organic matter either in the water column or in the sediments.

The relationship between the concentrations of (N+N) and SRP is shown in Fig. 15. When the data points from the inner shelf were excluded, they were linearly related to each other such that:

$$(\mathrm{N+N})\ (\mu\mathrm{M}) = 14.12(\pm 0.06)\mathrm{SRP} - 0.32(\pm 0.07) \quad N = 256;\ r^2 = 0.996$$

There was no significant seasonal difference in the relationship. Both the slope and the intercept were within the ranges found at the SEATS station in the northern South China Sea between 1999 and 2003 (Wong et al., 2007b). The slope, being smaller than the Redfield stoichiometric ratio of (N+N) to SRP of 16 (Redfield et al., 1963), reflected the effect of denitrification on the deep water while the small negative intercept was suggestive of (N+N) as the limiting nutrient. Some data points in both seasons from the inner shelf clearly fell away from this general relationship. They seemed to follow linear trends with steeper slopes. These indicate that these coastal waters were enriched in (N+N) relative to SRP. They likely represent the influence of the terrestrial sources to the NoSoCS that are known to be replete with (N+N) (Zhang, 1996; Dai et al., 2008; Liu et al., 2012). The enrichment in (N+N) was larger in the summer. This is consistent with the higher (N+N) to SRP ratios that were found during the summer months in the

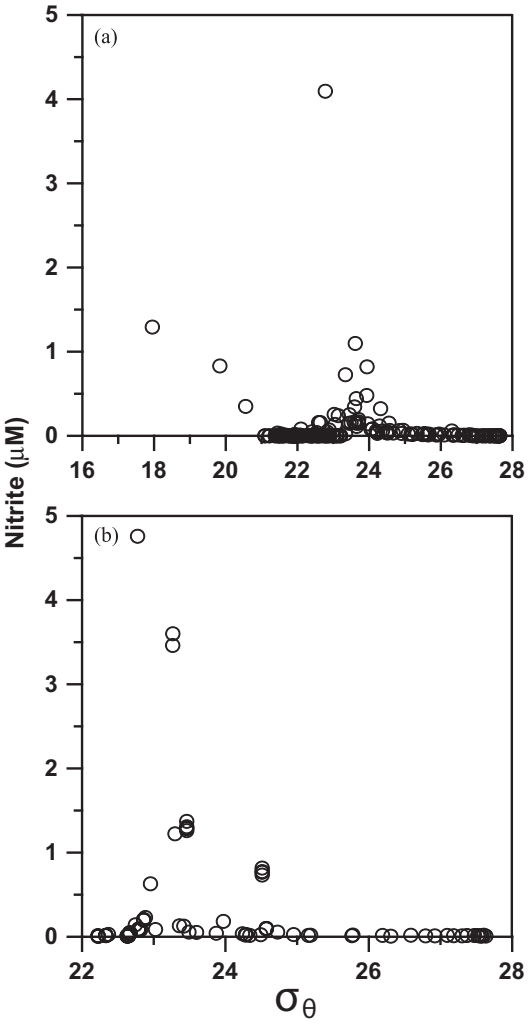

Fig. 14. The relationship between nitrite and potential density (σ_θ) in (a) the summer 2010 and (b) the winter 2011.

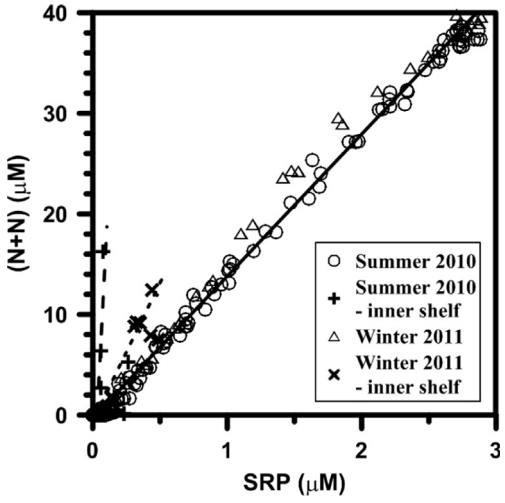

Fig. 15. The relationships between SRP and (N+N). ○ – summer, 2010; Δ – winter, 2011; + – inner shelf summer, 2010; x – inner shelf winter, 2011; solid line – best fit line when data points from the inner shelf were excluded.

surface water at the mouth of the Pearl River and that were closely related to the discharge of the Pearl River (Yin and Harrison, 2008; Xu et al., 2009).

3.4. (N+N)/SRP, nutrient anomaly (N^*), and excess nitrate ($[N+N]_{ex}$)

3.4.1. (N+N)/SRP, N^* and nitrogen fixation in the open SCS

The relative biogeochemical dynamics of (N+N) and SRP in the open ocean has been examined extensively by their concentration ratio, (N+N)/SRP and by the nitrate anomaly N^* (Fanning, 1992; Gruber and Sarmiento, 1997; Deutsch et al., 2001; Bates and Hansell, 2004; Hansell et al., 2004, 2007; Weber and Deutsch, 2010; Monteiro and Follows, 2012). N^* is defined as (Deutsch et al., 2001)

$$N^*(\mu M) = (N+N) - 16SRP + 2.90$$

If photosynthesis and respiration follow the stoichiometry in the Redfield model closely (Redfield et al., 1963), (N+N)/SRP is 16. Processes such as the preferential regeneration of SRP and denitrification may result in values below 16 while nitrogen fixation may lead to values above 16. If the effect of mixing can be neglected, N^* represents the deviation from the Redfield biological pump due to the combined effect of denitrification and nitrogen fixation. The global average deficit in (N+N) relative to SRP of 2.9 μM is inserted into the equation so that the global average N^* is taken to be about zero (Deutsch et al., 2001). A more positive value suggests a more dominant effect of nitrogen fixation over denitrification and vice versa.

N^* and (N+N)/SRP in the open northern SCS were calculated only from samples with concentrations of (N+N) >1 μM and SRP >0.1 μM in order to avoid the large uncertainties that are inherent in the determinations of low concentrations of (N+N) and SRP by the standard methods. Their relationships to potential density are shown in Fig. 16a and b. At depths below 600 m as σ_θ increased above 27, (N+N)/SRP converged to within a narrow range, between 13 and 15 in both seasons, while N^* were invariably <0 μM. They were indicative of the effects of denitrification as reported in the world's oceans (Deutsch et al., 2001). Between σ_θ of 25 and 27 in the upper nutricline between about 100–600 m, N^* turned positive, and some of the highest values of (N+N)/SRP, even exceeding 16, and N^*, reaching 4 μM, were found. These values of N^* were at the high end in the range of concentrations that had been reported in the world's oceans (Deutsch et al., 2001) and they were consistent with the effect of the remineralization of nitrogen-enriched organic matter formed by nitrogen fixation. Furthermore, both (N+N)/SRP and N^* were conspicuously higher in the winter than in the summer. If the elevated values were related to nitrogen fixation, these seasonal differences suggest that the effect of nitrogen fixation was more pronounced in the winter when atmospheric deposition of mineral dusts was the highest (Lin et al., 2007), and this is consistent with the stimulation of nitrogen fixation in oligotrophic waters by atmospherically derived iron (Capone et al., 1997). Wong and coworkers (Wong et al., 2002, 2007b) have examined the variations in N^* and (N+N)/SRP at a single location at the SEATS Station and the distribution of ^{15}N in (N+N) at a nearby location and hypothesized that nitrogen fixation occurs in the northern SCS and it may be more extensive between September and April when the atmospheric depositional flux of dusts is higher. The data reported here covered a wider geographic area and corroborated these findings well. At σ_θ of less than 25 in the top 100 m, (N+N)/SRP, ranging between 7 and 18, was highly variable and it did not follow a regular seasonal pattern while N^* stayed between 0 and 3 μM. At these shallower depths, other processes, such as the preferentially recycling of SRP over (N+N), could also have contributed to the relative dynamics of these two nutrients. Furthermore, the concentrations of (N+N) and SRP were relatively low at these depths. As a result, N^*, to a large extent, was no longer driven by the relative concentration differences between the two nutrients but by the global average deficit in (N+N) relative to SRP of 2.9 μM.

3.4.2. (N+N)/SRP, $[N+N]_{ex}$ and terrestrial nutrients in NoSoCS

In the shelf-seas, such as the NoSoCS, nitrogen fixation is unlikely to be an important process affecting the relative abundance of (N+N) and SRP as the nutrients tend to be more available and nitrogen fixation is thus suppressed in these waters. Indeed, Pan et al. (2013) reported that *Prochlorococcus*, a possible nitrogen fixing phytoplankton species, is seldom the dominant phytoplankton species in the NoSoCS. Thus, aside from primary production and respiration, the major processes that may affect the relative concentrations of (N+N) and SRP are their supplies from terrestrial inputs, exchanges with the sub-surface water in the open northern SCS and denitrification. (Atmospheric inputs of (N+N) and SRP to the NoSoCS are not well known but their influence is likely to be small. If the existing estimates to the SCS (Chen et al., 2001) are scaled to the area of the NoSoCS, they are equivalent to about 3% of the inputs from the Pearl River (Table 2).) Since the effects of these regional rather than global processes are the focus, the use of N^* to examine the relative dynamics of (N+N) and SRP may not be meaningful. Thus, Wong et al. (1998) devised 'excess nitrate', $[N+N]_{ex}$, for examining the influence of the terrestrial sources, especially the input from the (N+N)-rich Changjiang, on the nutrient dynamics in the surface waters of the East China Sea Shelf-sea such that:

$$[N+N]_{ex}\ (\mu M) = (N+N) - (R)SRP$$

In this approach, the nutrient concentrations in the sub-surface water from the open sea were used as the reference so that R is (N+N)/SRP in the upwelled water from the Kuroshio onto the East China Sea Shelf-sea. If the effects of primary production and respiration are assumed to be in an approximate balance, then, a positive $[N+N]_{ex}$ indicates that the influence of the (N+N)-replete terrestrial sources dominates over that of denitrification while a negative $[N+N]_{ex}$ may indicate the vice versa. This approach is taken here. Since there is free mixing between the NoSoCS and the open SCS below the mixed layer, the average ratio of (N+N) to SRP in the sub-surface layer below the mixed layer in the open SCS in the summer and winter, which can be estimated to be 13.8 ± 0.5 (Table 1), was used as R. The distributions of (N+N)/SRP and $[N+N]_{ex}$ in the transects across the NoSoCS are shown in Fig. 17. Conspicuously elevated values of (N+N)/SRP and $[N+N]_{ex}$, reaching maximum values of 220 and 15 μM respectively, were found in the fresher water in the inner shelf. These much elevated values reflected the dominating influence of the terrestrial inputs which were enriched in (N+N) over SRP (Zhang, 1996; Dai et al., 2008; Liu et al., 2012). In these waters where the ratio of (N+N)/SRP were substantially above 16, the Redfield stoichiometric ratio in photosynthetic activities and respiration (Redfield et al., 1963; Anderson and Sarmiento, 1994), SRP could have become the limiting nutrient (Xu et al., 2008, 2009). In the sub-surface water, there was inevitably a layer of bottom water with (N+N)/SRP < 13.8, the value in the source water from the open SCS, and $[N+N]_{ex} < 0$ μM covering some parts of the middle and outer shelf. These bottom waters with depressed values of (N+N)/SRP and $[N+N]_{ex}$ were consistent with the effect of denitrification and especially sedimentary denitrification.

The concentration of $[N+N]_{ex}$ was linearly related to salinity (Fig. 18a) such that:

$$[N+N]_{ex}\ (\mu M) = -2.64(\pm 0.14)S + 89.7(\pm 4.6) \quad N = 33;\ r^2 = 0.92$$

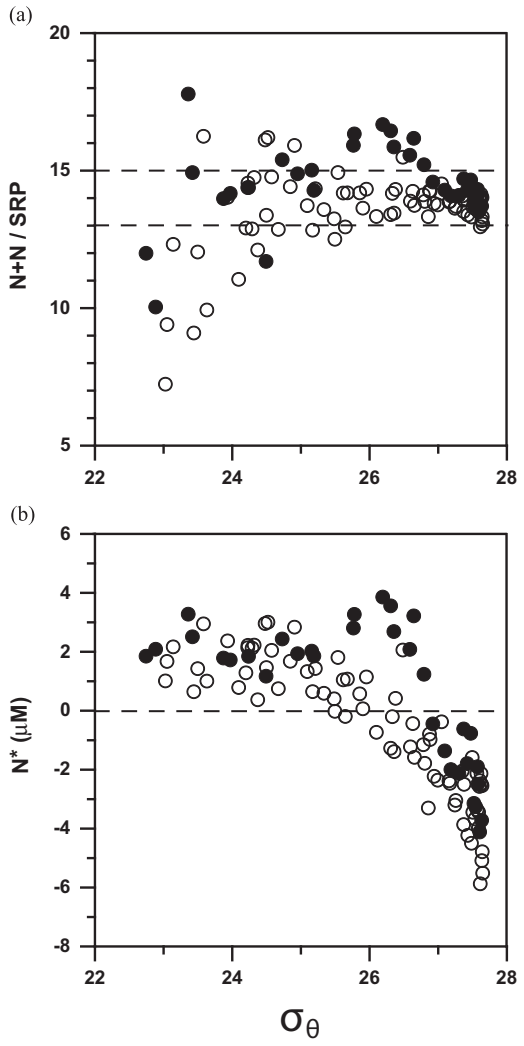

Fig. 16. The relationships between (a) (N+N)/SRP and (b) N^*, and, potential density (σ_θ) in the open SCS. o – summer, 2010; • – winter, 2011. Dashed lines in (a) denote range of values below ~600 m.

Table 2
Input values and results from a box modeling exercise on the dynamics of the nutrients in the mixed layer of the NoSoCS.

	Water flux ($m^3\ yr^{-1}$)	Salinity	SRP (μM)	SRP Flux ($mol\ yr^{-1}$)	(N+N) μM	(N+N) flux ($mol\ yr^{-1}$)
Inputs						
Pearl River	3.3×10^{11}(1)	0	2 ± 1 (2)	6.6×10^{8}	150 ± 100 (2)	4.95×10^{10}
Precipitation	3.84×10^{11} (3)	0	–	1.84×10^{7}(4)	–	1.43×10^{9} (4)
Net vertical mixing	4.21×10^{13}	34.25 ± 0.2	0.27 ± 0.03	1.14×10^{10}	3.05 ± 0.8	1.28×10^{11}
Outputs						
Evaporation	2.16×10^{11} (3)	0	0	0	0	0
Export to open SCS	4.26×10^{13}	33.85 ± 0.1	0.075 ± 0.04	3.19×10^{9}	1.0 ± 0.7	4.26×10^{10}
Biological removal	–	–	–	8.85×10^{9}	–	1.37×10^{11}

Area of NoSoCS – $1.61 \times 10^{11}\ m^2$; SRP – soluble reactive phosphate; (N+N) – (nitrate+nitrite). (1) Guo et al. (2008); (2) Dai et al. (2008); (3) Wong et al. (2007a); (4) area normalized flux from total flux to South China Sea of Chen et al. (2001).

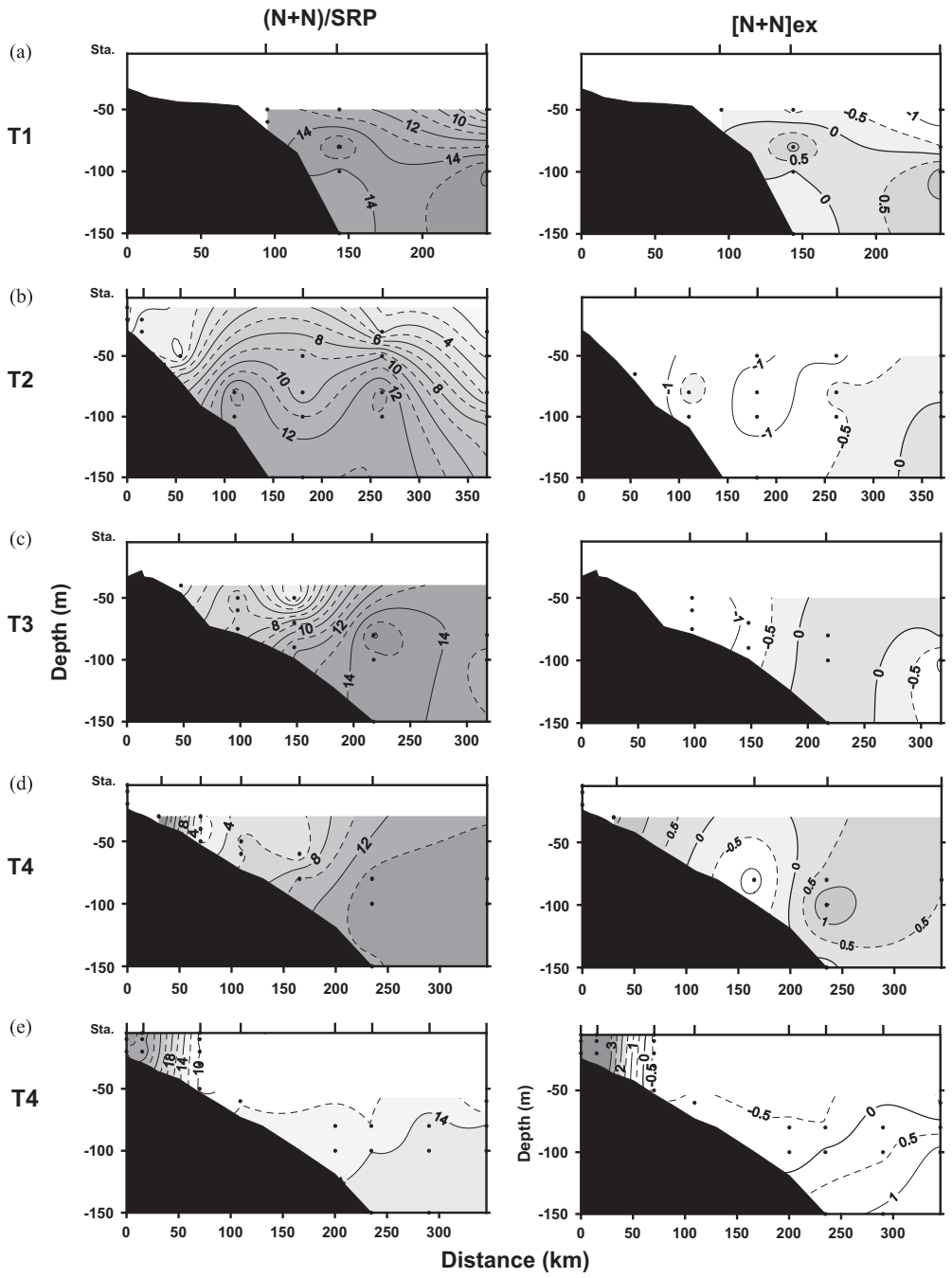

Fig. 17. The vertical sections of (N+N)/SRP and $[N+N]_{ex}$ across the shelf in transects (a) T1, (b) T2, (c) T3 and (d) T4 in the summer 2010, and (e) T4 in the winter 2011. Locations of the stations are shown at the top of the figures.

The linear relationship suggests that the composition of the shelf water could be represented by a two end-member mixing between the inner shelf water which was enriched with (N+N) and the bottom water on the shelf with a small deficit in (N+N). The relationship indicates that $[N+N]_{ex}$ reached 0 at a salinity of 33.9. Similarly, as a first approximation, (N+N)/SRP was also linearly related to salinity at salinities below 33 (Fig. 18b) such that:

$$(N+N)/SRP = -44.4(\pm 5.7)S + 1467(\pm 180) \quad N = 9;\ r^2 = 0.897$$

Thus, (N+N)/SRP was equal to 16 at a salinity of 32.7. Both of these relationships indicate that excess (N+N) over SRP could be found in waters with salinities below about 33. In these waters, if the two nutrients are used according to the Redfield ratio, SRP might become limiting eventually. However, waters with such low salinities were not commonly found in this study which was not conducted during a period of high runoff. These fresher waters were confined mostly to within the inner shelf. In contrast, while Wong et al. (1998) also found an approximately linear relationship between $[N+N]_{ex}$ and salinity in the East China Sea Shelf-sea, the waters with excess (N+N) covered about one-third to one half of that Shelf-sea.

3.5. *Assessing the nutrient dynamics and carbon fixation in the mixed layer of the NoSoCS*

A first order assessment of the dynamics of the nutrient elements in the mixed layer of the NoSoCS may be made in a simple box model exercise in which the NoSoCS is treated as a two layer system. Both layers can exchange freely with the open

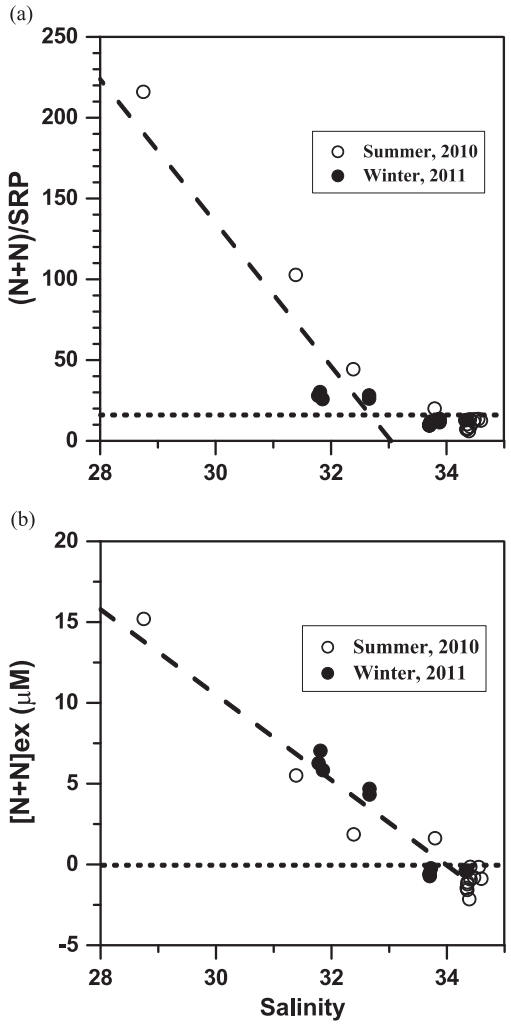

Fig. 18. The relationship between (a) (N+N)/SRP (short dashed line indicates the Redfield ratio of 16) and (b) $[N+N]_{ex}$ (short dashed line indicates $[N+N]_{ex}=0$), and salinity in the NoSoCS. o – summer 2010; • – winter 2011. Long dashed lines indicate the best fit lines at salinities below 33.

northern SCS but the exchanges with the Taiwan Strait and the Beibu Gulf are assumed to be minimal. Then, if a steady state exists, the inputs from river runoff, atmospheric deposition and vertical mixing of deep-water to the mixed layer in the NoSoCS are balanced by the net export from the NoSoCS to the open northern SCS as shown in Fig. 19. Thus, the material balances for water, salt, SRP and (N+N) in the mixed layer are given by

$$\text{Water balance}: \quad R+U+P=O+E \tag{1}$$

$$\text{Salt balance}: \quad R[S_r]+U[S_d]+P[S_p]=O[S_h]+E[S_e] \tag{2}$$

$$\text{SRP balance}: \quad R[P_r]+U[P_d]+P[P_p]=O[P_h]+E[P_e]+B_p \tag{3}$$

$$\text{(N+N) balance}: \quad R[N_r]+U[N_d]+P[N_p]=O[N_h]+E[N_e]+B_n \tag{4}$$

R, *U*, *P*, *O* and *E* are the water fluxes from riverine input, net vertical mixing, atmospheric precipitation, net outflow to the open northern SCS and evaporation respectively. The corresponding concentrations in these sources of material are denoted by the subscripts r, d, p, h and e. Salinity and the concentrations of SRP and combined inorganic nitrogen are given as S, P and N in square brackets, and B_p and B_n are the biological removal of SRP and (N+N) in net primary production. In the NoSoCS and the open northern SCS, combined inorganic nitrogen is treated as (N+N). In the river runoff and atmospheric deposition, ammonia is also included. The riverine input is assumed to originate virtually exclusively from the Pearl River, whose discharge, or *R*, is 330 $km^3\ yr^{-1}$ (Guo et al., 2008). *P* and *E* have been reported by the Hong Kong Observatory to be 2383 $mm\ yr^{-1}$ and 1343 $mm\ yr^{-1}$ respectively (Wong et al., 2007a). Salinity and the concentrations of the nutrients in the deep water and in the mixed layer are calculated as the averages of the summer and winter values given in Table 1. $[S_r]$, $[S_p]$ and $[S_e]$ are assumed to be negligible. The concentrations of SRP and (N+N) in the Pearl River water are estimated from Dai et al. (2008). The atmospheric depositional fluxes of SRP and (N+N) are estimated from the total fluxes to the South China Sea (Chen et al., 2001) after they have been scaled to the surface area of the NoSoCS. Then, after U and O have been calculated from the Eqs. (1) and (2), B_p and B_n may be estimated from Eqs. (3) and (4) respectively.

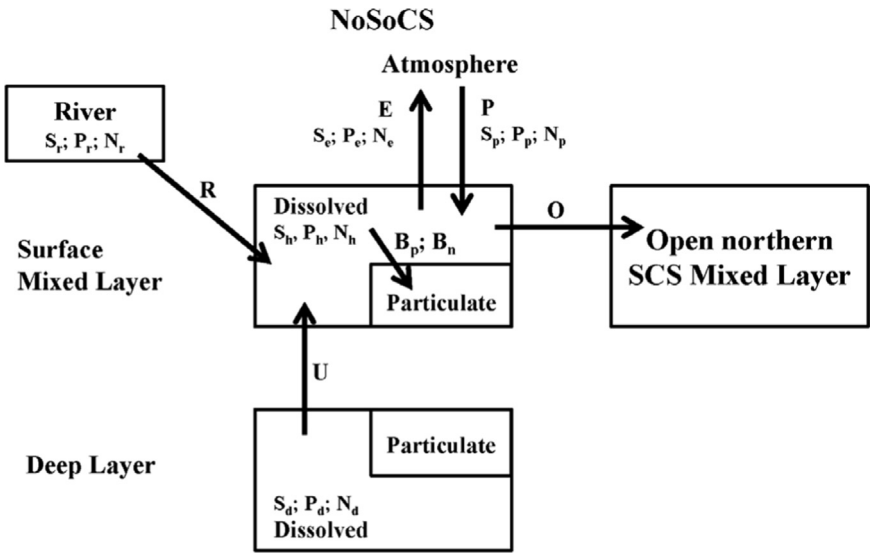

Fig. 19. A box model for the dynamics of the nutrients in the mixed layer in the NoSoCS. Symbols are defined in the text.

The input values and the results of this modeling exercise are given in Table 2. The results indicate that the input of water to the NoSoCS is dominated by vertical mixing as it contributes 98% of the total input to the mixed layer. Given that the average volume of the mixed layer over the two seasons is 6×10^{12} m^3, the residence time of the water in the mixed layer is about 2 months. This is a rather short residence time and suggests rigorous vertical mixing in the NoSoCS. Vertical mixing is also the dominant input of (N+N) and SRP to the mixed layer as it contributes 72% and 94% of their total input respectively. The riverine input of (N+N), 28% of the total input, is much more significant than that of SRP, which was equivalent to 5% of the total input. This reflects the enrichment of (N+N) over SRP in the Pearl River water. Biological utilization removes about 75% of both SRP and (N+N) added to the mixed layer. When the removals are converted to carbon fixation by using the Redfield ratio of 1:106 and 16:106 (Redfield et al., 1963), B_p and B_n yield similar carbon removal rates of 70 and 68 g-C m^{-2} yr^{-1}. Since these rates are supported by allochthanous nutrients, they represent new production. Through direct measurements, Chen and Chen (2006) reported that the average new production in NoSoCS in the spring, summer, fall and winter are 0.19, 0.15, 0.14 and 0.34 g-C m^{-2} d^{-1} respectively. These rates yield an average of 0.2 g-C m^{-2} d^{-1} or 75 g-C m^{-2} yr^{-1}. Pan et al. (2015) estimated through remotely sensed data that the net primary production in the NoSoCS is about 1.1 ± 0.7 g-C m^{-2} d^{-1}. By assuming an *f*-ratio of about 0.3 ± 0.1 in the NoSoCS (Chen and Chen, 2006), the corresponding new production would be 120 ± 75 g-C m^{-2} yr^{-1}. Given the uncertainties in the rates estimated from the box modeling exercise, they agree surprisingly well with these other independent estimations.

The results of this box modeling exercise are qualitatively insensitive to the range of the estimated average salinity and average concentrations of the nutrients in the different hydrographic sub-divisions listed in Tables 1 and 2. Using the maximum and minimum values would yield residence times of the water in the mixed layer of 2.1 and 1.3 months, the contribution of vertical mixing to the total input of (N+N) and SRP to the mixed layer of 61 and 88%, and, 91 and 97% respectively, the contribution of the biological removal of (N+N) and SRP added to the mixed layer of 73% and 88%, and 65% and 86%, and the corresponding carbon removal rates of 77 and 63, and 57 and 93 g-C m^{-2} yr^{-1}. Thus, the uncertainties in these estimations from the box modeling exercise are generally within about ±30%. Another source of uncertainties is the conceptual assumptions, such as the existence of a steady state in the NoSoCS, minimal exchanges between the NoSoCS and the Taiwan Strait and the Baibu Gulf, and only net exchanges between the mixed layers of the NoSoCS and the open SCS, and, between the surface and deep layer of the NoSoCS affect the mass balances of the nutrients. They cannot be assessed quantitatively by using the present data set. Their validity remains to be further tested.

4. Conclusions

Because of its shallow mixed layer depth, about 40 m in the summer and 70 m in the winter, the NoSoCS is permanently underlay by a layer of relatively nutrient-rich upper thermocline-upper nutricline water that extends freely into the Shelf-sea from the open SCS. Shelf-edge upwelling is unnecessary for bringing the nutrient-replete sub-surface water off the shelf to the NoSoCS. This is a distinguishing feature of the NoSoCS from many temperate shelf-seas. Vertical mixing on the shelf is a major control on the supply of nutrients to the mixed layer of NoSoCS as it contributes the majority of the total inputs of (N+N) and SRP to the mixed layer. This vertical mixing may be provided by: winter convective mixing by surface cooling, summer coastal upwelling at the northwestern corner of NoSoCS offshore of Shantou, the activities of internal waves along the outer and middle shelf year round, and the formation of bottom water in the winter.

Acknowledgments

This work was supported in part by the Ministry of Science and Technology, Taiwan through Grants NSC 101-2611-M-001-003-MY3 (to Wong) and NSC 101-2-811-M-001-083 (to Pan) and by the Academia Sinica, Taiwan through a post-doctoral fellowship (to Guo) and a thematic project grant titled “Ocean Acidification: Comparative biogeochemistry in shallow-water tropical coral reef ecosystems in a naturally acidic marine environment “ (to Wong, Shiah and Ho). This manuscript was completed while Wong was supported as a visiting professor at the Hong Kong University of Science and Technology and at the University of Malaya.

References

Anderson, L.A., Sarmiento, J.L., 1994. Redfield ratios of remineralization determined by nutrient data analysis. Glob. Biogeochem. Cycles 8, 65–80.
Bates, N.R., Hansell, D.A., 2004. Temporal variability of excess nitrate in the subtropical mode water of the North Atlantic Ocean. Mar. Chem. 84, 225–241.
Capone, D.G., Zehr, J.P., Paerl, H.W., Bergman, B., Carpenter, F.J., 1997. *Trichodesmium*, a globally significant marine cyanobacterium. Science 276, 122–1229.
Chao, S.Y., Shaw, P.T., Wu, S.Y., 1996. Deep water ventilation in the South China Sea. Deep-Sea Res. I 43, 445–466.
Chen, Y.-l. L., 2005. Spatial and seasonal variations of nitrate-based new production and primary production in the South China Sea. Deep-Sea Res. I 52, 319–340.
Chen, Y.-l. L., Chen, H.-Y., 2006. Seasonal dynamics of primary and new production in the northern South China Sea: the significance of river discharge and nutrient advection. Deep-Sea Res. I 53, 971–986.
Chen, C.-T.A., Wang, S.-L., 1999. Carbon, alkalinity and nutrient budget on the East China Sea continental shelf. J. Geophys. Res. 104, 20676–20686.
Chen, C.-T.A., Wang, S.-L., Wang, B.-J., Pai, S.-C., 2001. Nutrient budgets for the South China Sea basin. Mar. Chem. 75, 281–300.
Chen, Z., Li, Y., Pan, J., 2004. Distribution of colored dissolved organic matter and dissolved organic carbon in the Pearl River Estuary, China. Cont. Shelf Res. 24, 1845–1856.
Dai, M., Wang, L., Guo, X., Zhai, W., Li, Q., He, B., Kao, S.-J., 2008. Nitrification and inorganic nitrogen distribution in a large perturbed river/estuarine system: the Pearl River Estuary, China. Biogeosciences 5, 1227–1244.
Deutsch, S., Gruber, N., Key, R.M., Sarmiento, J.L., Ganachaud, A., 2001. Denitrification and N_2 fixation in the Pacific Ocean. Glob. Biogeochem. Cycles 15, 483–506.
Fanning, K.A., 1992. Nutrient provinces in the sea: concentration ratios, reaction rate ratios, and ideal covariation. J. Geophys. Res. 97 (C4), 5693–5712.
Gan, J., Li, H., Curchitser, E.N., Haidvogel, D.B., 2006. Modeling South China Sea circulation: response to seasonal forcing regimes. J. Geophys. Res. 111, C06034. http://dx.doi.org/10.1029/2005JC003298.
Gan, J., Cheung, A., Guo, X.G., Li, L., 2009. Intensified upwelling over a widened shelf in the northeastern South China Sea. J. Geophys. Res. 114, C09019. http://dx.doi.org/10.1029/2007JC004660.
Gan, J., Lu, Z., Dai, M., Cheung, A.Y.Y., Liu, H., Harrison, P., 2010. Biological response to intensified upwelling and to a river plume in the northeastern South China Sea: a modeling study. J. Geophys. Res. 115, C09001. http://dx.doi.org/10.1029/2009JC005569.
Gong, G.C., Liu, K.K., Liu, C.T., Pai, S.C., 1992. The chemical hydrography of the South China Sea west of Luzon and a comparison with the West Philippine Sea. Terr. Atmos. Ocean. Sci. 3, 587–602.
Gruber, N., Sarmiento, J.L., 1997. Global patterns of marine nitrogen fixation and denitrification. Glob. Biogeochem. Cycles 11 (2), 235–266.
Guo, X., Wong, G.T.F, 2015. Carbonate chemistry in the Northern South China Sea Shelf-Sea in June 2010. Deep-Sea Res. II, 117, 119–130. http://dx.doi.org/10.1016/j.dsr2.2015.02.024.
Guo, X., Cai, W.-J., Zhai, W., Dai, M., Wang., Y., Chen, B., 2008. Seasonal variations in the inorganic carbon system in the Pearl River (Zhujiang) estuary. Cont. Shelf Res. 28, 1424–1434.
Guo, C., Vlasenko, V., Alpers, W., Stashchuk, N., Chen, X., 2012. Evidence of short internal waves trailing strong internal solitary waves in the northern South China Sea from synthetic aperture radar obervations. Remote Sens. Environ. 124, 542–550.
Hansell, D.A., Bates, N.R., Olson, D.B., 2004. Excess nitrate and nitrogen fixation in the North Atlantic Ocean. Mar. Chem. 84, 243–265.
Hansell, D.A., Olson, D.B., Dentener, F., Zamora, L.M., 2007. Assessment of excess nitrate development in subtropical North Atlantic. Mar. Chem. 106, 562–579.

Harrison, P.J., Yin, K., Lee, J.H.W., Gan, J., Liu, H., 2008. Physical–biological coupling in the Pearl River Estuary. Cont. Shelf Res. 28, 1405–1415.
Heinrich, A.K., 1962. The life histories of plankton animals and seasonal cycles of plankton communities in the oceans. J. du Cons. Int. pour Exploration de la Mer 27, 15–24.
Hong, H., Chai, F., Zhang, C., Huang, B., Jiang, Y., Hu, J., 2011a. An overview of physical and biogeochemical processes and ecosystem dynamics in the Taiwan Strait. Cont. Shelf Res. 31, S3–S12.
Hong, H., Liu, X., Chiang, K.-P., Huang, B., Zhang, C., Hu, J., Li, Y., 2011b. The coupling of temporal and spatial variations of chlorophyll a concentration and the East Asian monsoons in the southern Taiwan Strait. Cont. Shelf Res. 31, S37–S47.
International Ocean-Colour Coordinating Group (IOCCG), 2000. Remote sensing of ocean color in coastal, and optically complex waters. In: Sathyendranath, S. (Ed.), Reports of the International Ocean-Colour Coordinating Group, Report 3, Dartmouth, N.S., Canada, 140 pp.
Karl, D.M., Tien, G., 1992. MAGIC: a sensitive and precise method for measuring dissolved phosphorus in aquatic environment. Limnol. Oceanogr. 37, 105–116.
Lee, T., Yoder, J., Atkinson, L., 1991. Gulf Stream frontal eddy influence on productivity of the southeast US continental shelf. J. Geophys. Res. 96, 22191–22205.
Lin, I.-I., Chen, J.-P., Wong, G.T.F., Huang, C.-W., Lien, C.-C., 2007. Aerosol input to the South China Sea: results from the Moderate Resolution Imaging Spectro-radiometer, the Quick Scatterometer, and the measurements of Pollution in the Troposphere Sensor. Deep-Sea Res. II 54, 1589–1601.
Liu, C.-T., Pinkel, R., Hsu, M.-K., Klymak, J.M., Chien, H.-W., Villanoy, C., 2006. Nonlinear internal waves from the Luzon Strait. EOS Trans. Am. Geophys. Union 87, 449–451.
Liu, Q., Dai, M., Chen, W., Huh, C.-A., Wang, G., Li, Q., Charette, M.A., 2012. How significant is submarine groundwater discharge and its associated dissolved inorganic carbon in a river-dominated shelf system? Biogeosciences 9, 1777–1795.
Montégut, C. de B., Madec, G., Fischer, A.S., Lazar, A., Iudicone, D., 2004. Mixed layer depth over the global ocean: an examination of profile data and a profile-based climatology. J. Geophys. Res. 109, C12003. http://dx.doi.org/10.1029/2004JC002378 (20 pp).
Monteiro, F.M., Follows, M.J., 2012. On nitrogen fixation and preferential reminer-alization of phosphorus. Geophys. Res. Lett. 39, L06607. http://dx.doi.org/10.1029/2012GL050897.
O'Reilly, J.E., Maritorena, S., Mitchell, B.G., Siegel, D.A., Carder, K.L., Garver, S.A., Kahru, M., McClain, C., 1998. Ocean color algorithms for SeaWiFS. J. Geophys. Res. 103 (C11), 24937–24953. http://dx.doi.org/10.1029/98JC02160.
O'Reilly, J.E., et al., 2000. SeaWiFS postlaunch calibration and validation analyses, part 3. In: Hooker, S.B., Firestone, E.R. (Eds.), SeaWiFS Postlaunch Technical Report Series, vol. 11, NASA Tech. Memo. 2000–206892. NASA Goddard Space Flight Center, Greenbelt, MD.
Pai, S.-C., Yang, C.-C., Riley, J.P., 1990. Formation kinetics of the pink azo dye in the determination of nitrite in natural waters. Anal. Chim. Acta 232, 345–349.
Pan, X., Mannino, A., Russ, M.E., Hooker, S.B., 2008. Remote sensing of the absorption coefficients and chlorophyll a concentration in the United States southern Middle Atlantic Bight from SeaWiFS and MODIS-Aqua. J. Geophys. Res. 113, C11022. http://dx.doi.org/10.1029/2008JC004852.
Pan, X., Wong, G.T.F., Shiah, F.-K., Ho, T.-Y., 2012. Enhancement of biological productivity by internal waves: observations in the summertime in the north-ern South China Sea. J. Oceanogr. 68, 427–437.
Pan, X., Wong, G.T.F., Ho, T.-Y., Shiah, F.-K., Liu, H., 2013. Remote sensing of picophytoplankton distribution in the northern South China Sea. Remote. Sens. Environ. 128, 162–175.
Pan, X., Wong, G.T.F., Tai, J.-H., Ho, T.-Y., 2015. Climatology of physical and biological characteristics of the northern South China Sea Shelf-sea (NoSoCS) and adjacent waters: observations from satellite remote sensing. Deep-Sea Res. II, 117, 10–22. http://dx.doi.org/10.1016/j.dsr2.2015.02.022.
Redfield, A.C., Ketchum, B.H., Richards, F.A., 1963. The influence of organisms on the composition of sea-water. In: Hill, M.N. (Ed.), The Sea, vol. 2. Interscience, New York, pp. 26–77.
Rimmelin, P., Moutin, T., 2005. Re-examination of the MAGIC method to determine low orthophosphate concentration in seawater. Anal. Chim. Acta 548 (1–2), 174–182.
Shang, S.L., Zhang, C.Y., Hong, H.S., Shang, S.P., Chai, F., 2004. Short-term variability of chlorophyll associated with upwelling events in the Taiwan Strait during the southwest monsoon of 1998. Deep-Sea Res. II 51, 1113–1127.
Strickland, J.D.H., Parsons, T.R., 1972. A Practical Handbook of Seawater Analysis, Bulletin 167, 2nd ed. Fisheries Research Board of Canada, Ottawa.
Szeto, M., Werdell, P.J., Moore, T.S., Campbell, J.W., 2011. Are the world's oceans optically different? J. Geophys. Res. 116, C00H04. http://dx.doi.org/10.1029/2011JC007230.
Tseng, C.-M., Wong, G.T.F., Lin, I.-I., Wu, C.-R., Liu, K.-K., 2005. A unique seasonal pattern in phytoplankton biomass in low-latitude waters in the South China Sea. Geophys. Res. Lett. 32, L08608. http://dx.doi.org/10.1029/2004GL022111.
Tseng, C.-M., Wong, G.T.F., Chou, W.-C., Lee, B.-S., Sheu, D.-D., Liu, K.-K., 2007. Temporal variations in the carbonate system in the upper layer at the SEATS station. Deep-Sea Res. II 54, 1448–1468. http://dx.doi.org/10.1016/j.dsr2.2007.05.003.
Tsunogai, S., Watanabe, S., Sato, T., 1999. Is there a "continental shelf pump" for the absorption of atmospheric CO_2? Tellus 51B, 701–712.
Wang, Y.-H., Dai, C.-F., Chen, Y.-Y., 2007. Physical and ecological processes of internal waves on an isolated reef ecosystem in the South China Sea. Geophys. Res. Lett. 34, L18609. http://dx.doi.org/10.1029/2007GL030658.
Weber, T.S., Deutsch, C., 2010. Ocean nutrient ratios governed by plankton biogeography. Nature 467, 550–554. http://dx.doi.org/10.1038/nature09403.
Wong, G.T.F., Pai, S.-C., Liu, K.-K., Liu, C.-T., Chen, G.-T.A., 1991. Variability of the chemical hydrography at the frontal region between the East China Sea and the Kuroshio north-east of Taiwan. Estuar. Coast. Shelf Sci. 33, 105–120.
Wong, G.T.F., Gong, G.-C., Liu, K.-K., Pai, S.-C., 1998. 'Excess nitrate' in the East China Sea. Estuar. Coast. Shelf Sci. 46, 411–418.
Wong, G.T.F., Chung, S.-W., Shiah, F.-K., Chen, C.-C., Wen, L.-S., Liu, K.-K., 2002. Nitrate anomaly in the upper nutricline in the northern South China Sea – evidence for nitrogen fixation. Geophys. Res. Lett. 29, 2097. http://dx.doi.org/10.1029/2002GL015796.
Wong, G.T.F., Hung, C.-C., Gong, G.-C., 2004. Dissolved iodine species in the East China Sea – a complementary tracer for upwelling water on the shelf. Cont. Shelf Res. 24, 1465–1484.
Wong, G.T.F., Ku, T.-L., Mulholland, M., Tseng, C.-M., Wang, D.-P., 2007a. The SouthEast Asian Time-series Study (SEATS) and the biogeochemistry of the South China Sea – an overview. Deep-Sea Res. II 54, 1434–1447.
Wong, G.T.F., Tseng, C.-M., Wen, L.-S., Chung, S.-W., 2007b. Nutrient dynamics and N-anomaly at the SEATS station. Deep-Sea Res. II 54, 1528–1545.
Xu, J., Yin, K., He, L., Yuan, X., Ho, A.Y.T., Harrison, P.J., 2008. Phosphorus limitation in the northern South China Sea during late summer: influence of the Pearl River. Deep-Sea Res. I 55, 1330–1342.
Xu, J., Yin, K., Ho, A.Y.T., Lee, J.H.W., Anderson, D.M., Harrison, P.J., 2009. Nutrient limitation in Hong Kong waters inferred from comparison of nutrient ratios, bioassays and ^{33}P turnover times. Mar. Ecol. Prog. Ser. 388, 81–97.
Yin, K., Harrison, P.J., 2008. Nitrogen over enrichment in subtropical Pearl River estuarine coastal waters: possible causes and consequences. Cont. Shelf Res. 28, 1435–1442.
Yin, K., Lin, Z., Ke, Z., 2004. Temporal and spatial distribution of dissolved oxygen in the Pearl River Estuary and adjacent coastal waters. Cont. Shelf Res. 24, 1935–1948.
Zhang, J., 1995. Geochemistry of trace metals from Chinese river/estuary systems: an overview. Estuar. Coast. Shelf Sci. 41, 631–658.
Zhang, J., 1996. Nutrient elements in large Chinese estuaries. Cont. Shelf Res. 16, 1023–1045.
Zheng, Q., Susanto, R.D., Ho, C.-R., Song, Y.T., Xu, Q., 2007. Statistical and dynamical analyses of generation mechanisms of solitary internal waves in the northern South China Sea. J. Geophys. Res. 112, C03021. http://dx.doi.org/10.1029/2006JC003551 (16 pp).